a possible association with Bcl-xL induction. Hepatology 1998;27:959–66.
105. Almeida OF, Conde GL, Crochemore C, Demeneix BA, Fischer D, Hassan AH, et al. Subtle shifts in the ratio between pro- and antiapoptotic molecules after activation of corticosteroid receptors decide neuronal fate. FASEB J 2000;14:779–90.
106. Hassan AH, von Rosenstiel P, Patchev VK, Holsboer F, Almeida OF. Exacerbation of apoptosis in the dentate gyrus of the aged rat by dexamethasone and the protective role of corticosterone. Exp Neurol 1996;140:43–52.
107. Hassan AH, Patchev VK, von Rosenstiel P, Holsboer F, Almeida OF. Plasticity of hippocampal corticosteroid receptors during aging in the rat. FASEB J 1999;13:115–22.
108. McCullers DL, Herman JP. Mineralocorticoid receptors regulate bcl-2 and p53 mRNA expression in hippocampus. Neuroreport 1998;9:3085–9.
109. Nishi M, Ogawa H, Ito T, Matsuda KI, Kawata M. Dynamic changes in subcellular localization of mineralocorticoid receptor in living cells: in comparison with glucocorticoid receptor using dual-color labeling with green fluorescent protein spectral variants. Mol Endocrinol 2001; 15:1077–92.
110. Sola S, Castro RE, Kren BT, Steer CJ, Rodrigues CM. Modulation of nuclear steroid receptors by ursodeoxycholic acid inhibits TGF-beta1-induced E2F-1/p53-mediated apoptosis of rat hepatocytes. Biochemistry 2004;43:8429–38.
111. Schwabe RF, Uchinami H, Qian T, Bennett BL, Lemasters JJ, Brenner DA. Differential requirement for c-Jun NH2-terminal kinase in TNFalpha- and Fas-mediated apoptosis in hepatocytes. FASEB J 2004;18:720–2.
112. Bailly-Maitre B, de Sousa G, Zucchini N, Gugenheim J, Boulukos KE, Rahmani R. Spontaneous apoptosis in primary cultures of human and rat hepatocytes: molecular mechanisms and regulation by dexamethasone. Cell Death Differ 2002;9:945–55.
113. Krueger A, Schmitz I, Baumann S, Krammer PH, Kirchhoff S. Cellular FLICE-inhibitory protein splice variants inhibit different steps of caspase-8 activation at the CD95 death-inducing signaling complex. J Biol Chem 2001;276: 20633–40.
114. Conticello C, Pedini F, Zeuner A, Patti M, Zerilli M, Stassi G, et al. IL-4 protects tumor cells from anti-CD95 and chemotherapeutic agents via up-regulation of antiapoptotic proteins. J Immunol 2004;172:5467–77.
115. Leverkus M, Neumann M, Mengling T, Rauch CT, Brocker EB, Krammer PH, et al. Regulation of tumor necrosis factor-related apoptosis-inducing ligand sensitivity in primary and transformed human keratinocytes. Cancer Res 2000;60:553–9.
116. Okano H, Shiraki K, Inoue H, Kawakita T, Yamanaka T, Deguchi M, et al. Cellular FLICE/caspase-8-inhibitory protein as a principal regulator of cell death and survival in human hepatocellular carcinoma. Lab Invest 2003;83: 1033–43.
117. Oh HY, Namkoong S, Lee SJ, Por E, Kim CK, Billiar TR, et al. Dexamethasone protects primary cultured hepatocytes from death receptor-mediated apoptosis by upregulation of cFLIP. Cell Death Differ 2006;13:512–23.
118. Bhadriraju K, Hansen LK. Extracellular matrix-dependent myosin dynamics during G1-S phase cell cycle progression in hepatocytes. Exp Cell Res 2004;300:259–71.
119. Coutant A, Rescan C, Gilot D, Loyer P, Guguen-Guillouzo C, Baffet G. PI3K-FRAP/mTOR pathway is critical for hepatocyte proliferation whereas MEK/ERK supports both proliferation and survival. Hepatology 2002;36:1079–88.
120. Iijima Y, Laser M, Shiraishi H, Willey CD, Sundaravadivel B, Xu L, et al. c-Raf/MEK/ERK pathway controls protein kinase C-mediated p70S6K activation in adult cardiac muscle cells. J Biol Chem 2002;277:23065–75.
121. Bessard A, Coutant A, Rescan C, Ezan F, Fremin C, Courselaud B, et al. An MLCK-dependent window in late G1 controls S phase entry of proliferating rodent hepatocytes via ERK-p70S6K pathway. Hepatology 2006; 44:152–63.
122. Suzuki YJ, Forman HJ, Sevanian A. Oxidants as stimulators of signal transduction. Free Radic Biol Med 1997;22: 269–85.
123. Carmody RJ, Cotter TG. Signalling apoptosis: a radical approach. Redox Rep 2001;6:77–90.
124. Ueda S, Masutani H, Nakamura H, Tanaka T, Ueno M, Yodoi J. Redox control of cell death. Antioxid Redox Signal 2002;4:405–14.
125. Suzuki YJ. Growth factor signaling for cardioprotection against oxidative stress-induced apoptosis. Antioxid Redox Signal 2003;5:741–9.
126. Matsuzawa A, Ichijo H. Stress-responsive protein kinases in redox-regulated apoptosis signaling. Antioxid Redox Signal 2005;7:472–81.
127. Culmsee C, Mattson MP. p53 in neuronal apoptosis. Biochem Biophys Res Commun 2005;331:761–77.
128. Shiba D, Shimamoto N. Attenuation of endogenous oxidative stress-induced cell death by cytochrome P450 inhibitors in primary cultures of rat hepatocytes. Free Radic Biol Med 1999;27:1019–26.
129. Ishihara Y, Shiba D, Shimamoto N. Primary hepatocyte apoptosis is unlikely to relate to caspase-3 activity under sustained endogenous oxidative stress. Free Radic Res 2005; 39:163–73.
130. Li LY, Luo X, Wang X. Endonuclease G is an apoptotic DNase when released from mitochondria. Nature 2001;412: 95–9.
131. Van Loo G, Schotte P, van Gurp M, Demol H, Hoorelbeke B, Gevaert K, et al. Endonuclease G: a mitochondrial protein released in apoptosis and involved in caspase-independent DNA degradation. Cell Death Differ 2001;8: 1136–42.
132. Ishihara Y, Shimamoto N. Involvement of endonuclease G in nucleosomal DNA fragmentation under sustained endogenous oxidative stress. J Biol Chem 2006;281:6726–33.
133. Ding Y, Le XP, Zhang QX, Du P. Methylation and mutation analysis of p16 gene in gastric cancer. World J Gastroenterol 2003;9:423–6.
134. Okano M, Bell DW, Haber DA, Li E. DNA methyltransferases Dnmt3a and Dnmt3b are essential for de novo methylation and mammalian development. Cell 1999;99: 247–57.
135. Xu J, Fan H, Zhao ZJ, Zhang JQ, Xie W. Identification of potential genes regulated by DNA methyltransferase 3B in a hepatocellular carcinoma cell line by RNA interference and microarray analysis. Yi Chuan Xue Bao 2005;32:1115–27.
136. Yin M, Wheeler MD, Kono H, Bradford BU, Gallucci RM, Luster MI, et al. Essential role of tumor necrosis factor alpha in alcohol-induced liver injury in mice. Gastroenterology 1999;117:942–52.
137. Bradham CA, Plumpe J, Manns MP, Brenner DA, Trautwein C. Mechanisms of hepatic toxicity. I. TNF-induced liver injury. Am J Physiol 1998;275:G387–92.
138. Slomiany BL, Piotrowski J, Slomiany A. Chronic alcohol ingestion enhances tumor necrosis factor-alpha expression and salivary gland apoptosis. Alcohol Clin Exp Res 1997;21: 1530–3.

139. Lin HZ, Yang SQ, Zeldin G, Diehl AM. Chronic ethanol consumption induces the production of tumor necrosis factor-alpha and related cytokines in liver and adipose tissue. Alcohol Clin Exp Res 1998;22:231S–7S.
140. Deaciuc IV, D'Souza NB, Spitzer JJ. Tumor necrosis factor-alpha cell-surface receptors of liver parenchymal and non-parenchymal cells during acute and chronic alcohol administration to rats. Alcohol Clin Exp Res 1995;19:332–8.
141. Pastorino JG, Hoek JB. Ethanol potentiates tumor necrosis factor-alpha cytotoxicity in hepatoma cells and primary rat hepatocytes by promoting induction of the mitochondrial permeability transition. Hepatology 2000;31:1141–52.
142. Fernandez-Checa JC, Kaplowitz N, Garcia-Ruiz C, Colell A, Miranda M, Mari M, et al. GSH transport in mitochondria: defense against TNF-induced oxidative stress and alcohol-induced defect. Am J Physiol 1997;273:G7–17.
143. Hatano E, Brenner DA. Akt protects mouse hepatocytes from TNF-alpha- and Fas-mediated apoptosis through NK-kappa B activation. Am J Physiol Gastrointest Liver Physiol 2001;281:G1357–68.
144. Kennedy SG, Kandel ES, Cross TK, Hay N. Akt/Protein kinase B inhibits cell death by preventing the release of cytochrome c from mitochondria. Mol Cell Biol 1999;19: 5800–10.
145. Khwaja A. Akt is more than just a Bad kinase. Nature 1999; 401:33–4.
146. Pastorino JG, Shulga N, Hoek JB. TNF-alpha-induced cell death in ethanol-exposed cells depends on p38 MAPK signaling but is independent of Bid and caspase-8. Am J Physiol Gastrointest Liver Physiol 2003;285:G503–16.
147. Shulga N, Hoek JB, Pastorino JG. Elevated PTEN levels account for the increased sensitivity of ethanol-exposed cells to tumor necrosis factor-induced cytotoxicity. J Biol Chem 2005;280:9416–24.
148. Akira S, Hemmi H. Recognition of pathogen-associated molecular patterns by TLR family. Immunol Lett 2003;85: 85–95.
149. Alexopoulou L, Holt AC, Medzhitov R, Flavell RA. Recognition of double-stranded RNA and activation of NF-kappaB by Toll-like receptor 3. Nature 2001;413:732–8.
150. Hoebe K, Du X, Georgel P, Janssen E, Tabeta K, Kim SO, et al. Identification of Lps2 as a key transducer of MyD88-independent TIR signalling. Nature 2003;424:743–8.
151. Oshiumi H, Matsumoto M, Funami K, Akazawa T, Seya T. TICAM-1, an adaptor molecule that participates in Toll-like receptor 3-mediated interferon-beta induction. Nat Immunol 2003;4:161–7.
152. Yamamoto M, Sato S, Mori K, Hoshino K, Takeuchi O, Takeda K, et al. Cutting edge: a novel Toll/IL-1 receptor domain-containing adapter that preferentially activates the IFN-beta promoter in the Toll-like receptor signaling. J Immunol 2002;169:6668–72.
153. Yamamoto M, Sato S, Hemmi H, Hoshino K, Kaisho T, Sanjo H, et al. Role of adaptor TRIF in the MyD88-independent toll-like receptor signaling pathway. Science 2003;301:640–3.
154. Lund JM, Alexopoulou L, Sato A, Karow M, Adams NC, Gale NW, et al. Recognition of single-stranded RNA viruses by Toll-like receptor 7. Proc Natl Acad Sci U S A 2004;101: 5598–603.
155. Honda K, Sakaguchi S, Nakajima C, Watanabe A, Yanai H, Matsumoto M, et al. Selective contribution of IFN-alpha/beta signaling to the maturation of dendritic cells induced by double-stranded RNA or viral infection. Proc Natl Acad Sci U S A 2003;100:10872–7.
156. Edelmann KH, Richardson-Burns S, Alexopoulou L, Tyler KL, Flavell RA, Oldstone MB. Does Toll-like receptor 3 play a biological role in virus infections? Virology 2004;322: 231–8.
157. Yoneyama M, Kikuchi M, Natsukawa T, Shinobu N, Imaizumi T, Miyagishi M, et al. The RNA helicase RIG-I has an essential function in double-stranded RNA-induced innate antiviral responses. Nat Immunol 2004;5:730–7.
158. Li K, Chen Z, Kato N, Gale M Jr, Lemon SM. Distinct poly(I-C) and virus-activated signaling pathways leading to interferon-beta production in hepatocytes. J Biol Chem 2005;280:16739–47.
159. Noguchi M, Hirohashi S. Cell lines from non-neoplastic liver and hepatocellular carcinoma tissue from a single patient. In Vitro Cell Dev Biol Anim 1996;32:135–7.
160. Ikeda M, Sugiyama K, Mizutani T, Tanaka T, Tanaka K, Sekihara H, et al. Human hepatocyte clonal cell lines that support persistent replication of hepatitis C virus. Virus Res 1998;56:157–67.
161. Arima N, Kao CY, Licht T, Padmanabhan R, Sasaguri Y, Padmanabhan R. Modulation of cell growth by the hepatitis C virus nonstructural protein NS5A. J Biol Chem 2001;276: 12675–84.
162. Kato N. Molecular virology of hepatitis C virus. Acta Med Okayama 2001;55:133–59.
163. Ray RB, Ray R. Hepatitis C virus core protein: intriguing properties and functional relevance. FEMS Microbiol Lett 2001;202:149–56.
164. Reed KE, Rice CM. Overview of hepatitis C virus genome structure, polyprotein processing, and protein properties. Curr Top Microbiol Immunol 2000;242:55–84.
165. Dubourdeau M, Miyamura T, Matsuura Y, Alric L, Pipy B, Rousseau D. Infection of HepG2 cells with recombinant adenovirus encoding the HCV core protein induces p21(WAF1) down-regulation—effect of transforming growth factor beta. J Hepatol 2002;37:486–92.
166. Jung EY, Lee MN, Yang HY, Yu D, Jang KL. The repressive activity of hepatitis C virus core protein on the transcription of p21(waf1) is regulated by protein kinase A-mediated phosphorylation. Virus Res 2001;79:109–15.
167. Lu W, Lo SY, Chen M, Wu K, Fung YK, Ou JH. Activation of p53 tumor suppressor by hepatitis C virus core protein. Virology 1999;264:134–41.
168. Marusawa H, Hijikata M, Chiba T, Shimotohno K. Hepatitis C virus core protein inhibits Fas- and tumor necrosis factor alpha-mediated apoptosis via NF-kappaB activation. J Virol 1999;73:4713–20.
169. Ray RB, Steele R, Meyer K, Ray R. Hepatitis C virus core protein represses p21WAF1/Cip1/Sid1 promoter activity. Gene 1998;208:331–6.
170. Scholle F, Li K, Bodola F, Ikeda M, Luxon BA, Lemon SM. Virus-host cell interactions during hepatitis C virus RNA replication: impact of polyprotein expression on the cellular transcriptome and cell cycle association with viral RNA synthesis. J Virol 2004;78:1513–24.
171. Tsuchihara K, Hijikata M, Fukuda K, Kuroki T, Yamamoto N, Shimotohno K. Hepatitis C virus core protein regulates cell growth and signal transduction pathway transmitting growth stimuli. Virology 1999;258:100–7.
172. Dansako H, Naganuma A, Nakamura T, Ikeda F, Nozaki A, Kato N. Differential activation of interferon-inducible genes by hepatitis C virus core protein mediated by the interferon stimulated response element. Virus Res 2003;97:17–30.
173. Naganuma A, Nozaki A, Tanaka T, Sugiyama K, Takagi H, Mori M, et al. Activation of the interferon-inducible 2′-5′-oligoadenylate synthetase gene by hepatitis C virus core protein. J Virol 2000;74:8744–50.

174. Naganuma A, Dansako H, Nakamura T, Nozaki A, Kato N. Promotion of microsatellite instability by hepatitis C virus core protein in human non-neoplastic hepatocyte cells. Cancer Res 2004;64:1307–14.
175. Naka K, Dansako H, Kobayashi N, Ikeda M, Kato N. Hepatitis C virus NS5B delays cell cycle progression by inducing interferon-beta via Toll-like receptor 3 signaling pathway without replicating viral genomes. Virology 2006; 346:348–62.
176. MacDonald G, Shi L, Vande Velde C, Lieberman J, Greenberg AH. Mitochondria-dependent and -independent regulation of Granzyme B-induced apoptosis. J Exp Med 1999; 189:131–44.
177. Song E, Chen J, Su F, Wang M, Heemann U. Granzyme B inhibitor I reduces apoptotic cell death of allogeneic-transplanted hepatocytes in spleen. Transplant Proc 2001; 33:3274–5.
178. Wang J, Li W, Min J, Ou Q, Chen J. Fas siRNA reduces apoptotic cell death of allogeneic-transplanted hepatocytes in mouse spleen. Transplant Proc 2003;35:1594–5.
179. Kondo T, Suda T, Fukuyama H, Adachi M, Nagata S. Essential roles of the Fas ligand in the development of hepatitis. Nat Med 1997;3:409–13.
180. Kuhnel F, Zender L, Paul Y, Tietze MK, Trautwein C, Manns M, et al. NFkappaB mediates apoptosis through transcriptional activation of Fas (CD95) in adenoviral hepatitis. J Biol Chem 2000;275:6421–7.
181. Mundt B, Kuhnel F, Zender L, Paul Y, Tillmann H, Trautwein C, et al. Involvement of TRAIL and its receptors in viral hepatitis. FASEB J 2003;17:94–6.
182. Shi Y. Mechanisms of caspase activation and inhibition during apoptosis. Mol Cell 2002;9:459–70.
183. Nishimura Y, Hirabayashi Y, Matsuzaki Y, Musette P, Ishii A, Nakauchi H, et al. In vivo analysis of Fas antigen-mediated apoptosis: effects of agonistic anti-mouse Fas mAb on thymus, spleen and liver. Int Immunol 1997;9:307–16.
184. Zender L, Hutker S, Liedtke C, Tillmann HL, Zender S, Mundt B, et al. Caspase 8 small interfering RNA prevents acute liver failure in mice. Proc Natl Acad Sci U S A 2003; 100:7797–802.
185. Kanzler S, Galle PR. Apoptosis and the liver. Semin Cancer Biol 2000;10:173–84.
186. Eichhorst ST. Modulation of apoptosis as a target for liver disease. Expert Opin Ther Targets 2005;9:83–99.
187. Gressner AM, Weiskirchen R. The tightrope of therapeutic suppression of active transforming growth factor-beta: high enough to fall deeply? J Hepatol 2003;39:856–9.
188. Mizuguchi Y, Yokomuro S, Mishima T, Arima Y, Shimizu T, Kawahigashi Y, et al. Short hairpin RNA modulates transforming growth factor beta signaling in life-threatening liver failure in mice. Gastroenterology 2005;129:1654–62.
189. Rust C, Gores GJ. Apoptosis and liver disease. Am J Med 2000;108:567–74.
190. Siegel RM, Fleisher TA. The role of Fas and related death receptors in autoimmune and other disease states. J Allergy Clin Immunol 1999;103:729–38.
191. Canbay A, Higuchi H, Bronk SF, Taniai M, Sebo TJ, Gores GJ. Fas enhances fibrogenesis in the bile duct ligated mouse: a link between apoptosis and fibrosis. Gastroenterology 2002;123:1323–30.
192. Galle PR, Hofmann WJ, Walczak H, Schaller H, Otto G, Stremmel W, et al. Involvement of the CD95 (APO-1/Fas) receptor and ligand in liver damage. J Exp Med 1995;182: 1223–30.
193. Li XK, Fujino M, Sugioka A, Morita M, Okuyama T, Guo L, et al. Fulminant hepatitis by Fas-ligand expression in MRL-lpr/lpr mice grafted with Fas-positive livers and wild-type mice with Fas-mutant livers. Transplantation 2001;71: 503–8.
194. Song E, Lee SK, Wang J, Ince N, Ouyang N, Min J, et al. RNA interference targeting Fas protects mice from fulminant hepatitis. Nat Med 2003;9:347–51.
195. Bartenschlager R, Frese M, Pietschmann T. Novel insights into hepatitis C virus replication and persistence. Adv Virus Res 2004;63:71–180.
196. Randall G, Rice CM. Hepatitis C virus cell culture replication systems: their potential use for the development of antiviral therapies. Curr Opin Infect Dis 2001;14: 743–7.
197. Zeuzem S, Feinman SV, Rasenack J, Heathcote EJ, Lai MY, Gane E, et al. Peginterferon alfa-2a in patients with chronic hepatitis C. N Engl J Med 2000;343:1666–72.
198. Heathcote EJ, Shiffman ML, Cooksley WG, Dusheiko GM, Lee SS, Balart L, et al. Peginterferon alfa-2a in patients with chronic hepatitis C and cirrhosis. N Engl J Med 2000;343: 1673–80.
199. Kato N, Hijikata M, Ootsuyama Y, Nakagawa M, Ohkoshi S, Sugimura T, et al. Molecular cloning of the human hepatitis C virus genome from Japanese patients with non-A, non-B hepatitis. Proc Natl Acad Sci U S A 1990;87:9524–8.
200. Bartenschlager R, Lohmann V. Replication of hepatitis C virus. J Gen Virol 2000;81:1631–48.
201. Thomas DL. Hepatitis C epidemiology. Curr Top Microbiol Immunol 2000;242:25–41.
202. McHutchison JG, Patel K. Future therapy of hepatitis C. Hepatology 2002;36:S245–52.
203. Kim WR. The burden of hepatitis C in the United States. Hepatology 2002;36:S30–4.
204. McHutchison JG. Hepatitis C advances in antiviral therapy: what is accepted treatment now? J Gastroenterol Hepatol 2002;17:431–41.
205. McCaffrey AP, Meuse L, Pham TT, Conklin DS, Hannon GJ, Kay MA. RNA interference in adult mice. Nature 2002; 418:38–9.
206. Wilson JA, Jayasena S, Khvorova A, Sabatinos S, Rodrigue-Gervais IG, Arya S, et al. RNA interference blocks gene expression and RNA synthesis from hepatitis C replicons propagated in human liver cells. Proc Natl Acad Sci U S A 2003;100:2783–8.
207. Wilson JA, Richardson CD. Hepatitis C virus replicons escape RNA interference induced by a short interfering RNA directed against the NS5b coding region. J Virol 2005; 79:7050–8.
208. Kapadia SB, Brideau-Andersen A, Chisari FV. Interference of hepatitis C virus RNA replication by short interfering RNAs. Proc Natl Acad Sci U S A 2003;100:2014–8.
209. Randall G, Grakoui A, Rice CM. Clearance of replicating hepatitis C virus replicon RNAs in cell culture by small interfering RNAs. Proc Natl Acad Sci U S A 2003;100:235–40.
210. Blight KJ, McKeating JA, Rice CM. Highly permissive cell lines for subgenomic and genomic hepatitis C virus RNA replication. J Virol 2002;76:13001–14.
211. Choo QL, Richman KH, Han JH, Berger K, Lee C, Dong C, et al. Genetic organization and diversity of the hepatitis C virus. Proc Natl Acad Sci U S A 1991;88:2451–5.
212. Okamoto H, Okada S, Sugiyama Y, Kurai K, Iizuka H, Machida A, et al. Nucleotide sequence of the genomic RNA of hepatitis C virus isolated from a human carrier: comparison with reported isolates for conserved and divergent regions. J Gen Virol 1991;72:2697–704.
213. Yokota T, Sakamoto N, Enomoto N, Tanabe Y, Miyagishi M, Maekawa S, et al. Inhibition of intracellular hepatitis C

virus replication by synthetic and vector-derived small interfering RNAs. EMBO Rep 2003;4:602–8.
214. Kronke J, Kittler R, Buchholz F, Windisch MP, Pietschmann T, Bartenschlager R, et al. Alternative approaches for efficient inhibition of hepatitis C virus RNA replication by small interfering RNAs. J Virol 2004;78:3436–46.
215. Takigawa Y, Nagano-Fujii M, Deng L, Hidajat R, Tanaka M, Mizuta H, et al. Suppression of hepatitis C virus replicon by RNA interference directed against the NS3 and NS5B regions of the viral genome. Microbiol Immunol 2004;48: 591–8.
216. Kruger M, Beger C, Welch PJ, Barber JR, Manns MP, Wong-Staal F. Involvement of proteasome alpha-subunit PSMA7 in hepatitis C virus internal ribosome entry site-mediated translation. Mol Cell Biol 2001;21:8357–64.
217. Ma WJ, Cheng S, Campbell C, Wright A, Furneaux H. Cloning and characterization of HuR, a ubiquitously expressed Elav-like protein. J Biol Chem 1996;271:8144–51.
218. Spangberg K, Wiklund L, Schwartz S. HuR, a protein implicated in oncogene and growth factor mRNA decay, binds to the 3′ ends of hepatitis C virus RNA of both polarities. Virology 2000;274:378–90.
219. Korf M, Jarczak D, Beger C, Manns MP, Kruger M. Inhibition of hepatitis C virus translation and subgenomic replication by siRNAs directed against highly conserved HCV sequence and cellular HCV cofactors. J Hepatol 2005; 43:225–34.
220. Gomez-Gonzalo M, Carretero M, Rullas J, Lara-Pezzi E, Aramburu J, Berkhout B, et al. The hepatitis B virus X protein induces HIV-1 replication and transcription in synergy with T-cell activation signals: functional roles of NF-kappaB/NF-AT and SP1-binding sites in the HIV-1 long terminal repeat promoter. J Biol Chem 2001;276: 35435–43.
221. Gong G, Waris G, Tanveer R, Siddiqui A. Human hepatitis C virus NS5A protein alters intracellular calcium levels, induces oxidative stress, and activates STAT-3 and NF-kappa B. Proc Natl Acad Sci U S A 2001;98:9599–604.
222. Matskevich AA, Strayer DS. Exploiting hepatitis C virus activation of NFkappaB to deliver HCV-responsive expression of interferons alpha and gamma. Gene Ther 2003;10: 1861–73.
223. Strayer DS, Feitelson M, Sun B, Matskevich AA. Paradigms for conditional expression of RNA interference molecules for use against viral targets. Methods Enzymol 2005;392: 227–41.
224. Hamazaki H, Ujino S, Miyano-Kurosaki N, Shimotohno K, Takaku H. Inhibition of hepatitis C virus RNA replication by short hairpin RNA synthesized by T7 RNA polymerase in hepatitis C virus subgenomic replicons. Biochem Biophys Res Commun 2006;343:988–94.
225. Seeger C, Mason WS. Hepatitis B virus biology. Microbiol Mol Biol Rev 2000;64:51–68.
226. Beasley RP, Hwang LY, Lin CC, Chien CS. Hepatocellular carcinoma and hepatitis B virus. A prospective study of 22 707 men in Taiwan. Lancet 1981;2:1129–33.
227. Dienstag JL, Perrillo RP, Schiff ER, Bartholomew M, Vicary C, Rubin M. A preliminary trial of lamivudine for chronic hepatitis B infection. N Engl J Med 1995;333:1657–61.
228. Hadziyannis SJ, Tassopoulos NC, Heathcote EJ, Chang TT, Kitis G, Rizzetto M, et al. Long-term therapy with adefovir dipivoxil for HBeAg-negative chronic hepatitis B. N Engl J Med 2005;352:2673–81.
229. Liaw YF, Sung JJ, Chow WC, Farrell G, Lee CZ, Yuen H, et al. Lamivudine for patients with chronic hepatitis B and advanced liver disease. N Engl J Med 2004;351:1521–31.
230. Marcellin P, Lau GK, Bonino F, Farci P, Hadziyannis S, Jin R, et al. Peginterferon alfa-2a alone, lamivudine alone, and the two in combination in patients with HBeAg-negative chronic hepatitis B. N Engl J Med 2004;351:1206–17.
231. Manesis EK, Hadziyannis SJ. Interferon alpha treatment and retreatment of hepatitis B e antigen-negative chronic hepatitis B. Gastroenterology 2001;121:101–9.
232. McCaffrey AP, Nakai H, Pandey K, Huang Z, Salazar FH, Xu H, et al. Inhibition of hepatitis B virus in mice by RNA interference. Nat Biotechnol 2003;21:639–44.
233. Giladi H, Ketzinel-Gilad M, Rivkin L, Felig Y, Nussbaum O, Galun E. Small interfering RNA inhibits hepatitis B virus replication in mice. Mol Ther 2003;8:769–76.
234. Konishi M, Wu CH, Wu GY. Inhibition of HBV replication by siRNA in a stable HBV-producing cell line. Hepatology 2003;38:842–50.
235. Shlomai A, Shaul Y. Inhibition of hepatitis B virus expression and replication by RNA interference. Hepatology 2003; 37:764–70.
236. Hamasaki K, Nakao K, Matsumoto K, Ichikawa T, Ishikawa H, Eguchi K. Short interfering RNA-directed inhibition of hepatitis B virus replication. FEBS Lett 2003;543:51–4.
237. Ying C, De Clercq E, Neyts J. Selective inhibition of hepatitis B virus replication by RNA interference. Biochem Biophys Res Commun 2003;309:482–4.
238. Klein C, Bock CT, Wedemeyer H, Wustefeld T, Locarnini S, Dienes HP, et al. Inhibition of hepatitis B virus replication in vivo by nucleoside analogues and siRNA. Gastroenterology 2003;125:9–18.
239. Chen Y, Du D, Wu J, Chan CP, Tan Y, Kung HF, et al. Inhibition of hepatitis B virus replication by stably expressed shRNA. Biochem Biophys Res Commun 2003;311:398–404.
240. Wu Y, Huang AL, Tang N, Zhang BQ, Lu NF. Specific antiviral effects of RNA interference on replication and expression of hepatitis B virus in mice. Chin Med J (Engl) 2005; 118:1351–6.
241. Morrissey DV, Blanchard K, Shaw L, Jensen K, Lockridge JA, Dickinson B, et al. Activity of stabilized short interfering RNA in a mouse model of hepatitis B virus replication. Hepatology 2005;41:1349–56.
242. Morrissey DV, Lockridge JA, Shaw L, Blanchard K, Jensen K, Breen W, et al. Potent and persistent in vivo anti-HBV activity of chemically modified siRNAs. Nat Biotechnol 2005;23:1002–7.
243. Uprichard SL, Boyd B, Althage A, Chisari FV. Clearance of hepatitis B virus from the liver of transgenic mice by short hairpin RNAs. Proc Natl Acad Sci U S A 2005;102:773–8.
244. Wu HL, Huang LR, Huang CC, Lai HL, Liu CJ, Huang YT, et al. RNA interference-mediated control of hepatitis B virus and emergence of resistant mutant. Gastroenterology 2005;128:708–16.
245. Carmona S, Ely A, Crowther C, Moolla N, Salazar FH, Marion PL, et al. Effective inhibition of HBV replication in vivo by anti-HBx short hairpin RNAs. Mol Ther 2006;13: 411–21.
246. Kim YH, Lee JH, Paik NW, Rho HM. RNAi-based knockdown of HBx mRNA in HBx-transformed and HBV-producing human liver cells. DNA Cell Biol 2006; 25:412–7.
247. Chen CC, Ko TM, Ma HI, Wu HL, Xiao X, Li J, et al. Long-term inhibition of hepatitis B virus in transgenic mice by double-stranded adeno-associated virus 8-delivered short hairpin RNA. Gene Ther 2007;14:11–9.

Biosci. Biotechnol. Biochem., **71** (12), 3082–3089, 2007

Annexin A3-Expressing Cellular Phenotypes Emerge from Necrotic Lesion in the Pericentral Area in 2-Acetylaminofluoren/Carbon Tetrachloride-Treated Rat Livers

Yoshimasa Ito,[1] Takenori Watanabe,[1] Shunsuke Nagatomo,[1] Taiichiro Seki,[1,†] Shingo Niimi,[2] and Toyohiko Ariga[1]

[1]*Laboratory of Nutrition and Physiology, Department of Agricultural and Biological Chemistry, Nihon University College of Bioresource Sciences, Fujisawa, Kanagawa 252-8510, Japan*
[2]*Division of Biological Chemistry and Biologicals, National Institute of Health Sciences, Kamiyoga, Tokyo 158-8501, Japan*

Received August 7, 2007; Accepted September 11, 2007; Online Publication, December 7, 2007
[doi:10.1271/bbb.70501]

Recently we found a small hepatocyte-specific protein, annexin A3 (AnxA3), in fractionated adult rat hepatocytes. Here we describe the results of an *in vivo* demonstration of AnxA3-expressing cellular phenotypes in the liver with 2-acetylaminofluoren (2-AAF)/carbon tetrachloride (CCl_4)-injury. In association with an elevation of alanine amino transferase (ALT) and aspartic acid amino transferase (AST) activities, hepatic AnxA3 mRNA increased markedly. AnxA3-positive cells were detected in clustered cells present in or emerging from the pericentral region. These albumin-expressed cells were histologically similar to cells expressing CD34, a hematopoietic cell marker protein. The number of clusters decreased in the days following CCl_4 treatment, and annexin-negative, but albumin-positive, oval cells appeared. We concluded that the agent-induced liver defect initially recruits bone marrow-derived cells, and that it promotes differentiation of these cells into AnxA3-positive cells, followed by emergence of the oval cells, which might have a role in the restitution of the damaged liver.

Key words: small hepatocyte; oval cell; annexin A3; liver regeneration; 2-acetylaminofluoren

The liver plays central roles in the metabolism of nutrients, production of plasma proteins, detoxification of xenobiotics and so on. The liver precisely maintains its mass when it receives surgical resection of hepatic lobes or undergoes loss of hepatocytes by viral infection or by cytotoxic chemicals. Regeneration of the liver is performed by the extraordinarily high replicative potency of parenchymal hepatocytes and biliary epithelial cells,[1,2] but in some pathological livers that suffer suppressed hepatocyte proliferation, other participants arise either from inside or outside the liver contributing to immediate rebuilding of the organ.[3–7] Of these participants, oval cells are known to emerge from a locus in the canal of Hering following chronic liver injury,[8] and they work as a kind of stem cells with their bipotential capacity to become either hepatocytes or biliary ducts.[9–11] On the other hand, small hepatocytes, a hepatic cell fraction of smaller size (approximately 17 μm in diameter) and, with higher proliferating potential than the majority of hepatocytes, are assumed to be another candidate for hepatocyte progenitor.[12,13] The origin of small hepatocytes, however, remains controversial. In cell culture experiments using human and animal hepatocytes, researchers isolate small hepatocyte-like progenitor cells in these isolated hepatocytes,[12,14] whereas in *in vivo* experiments using anti-mitotic or anti-replicative agents such as 2-AAF or retrorsine, they observe oval cells as a progenitor of small hepatocytes.[15,16] There is an old finding that both oval cells and small hepatocytes can be generated from duct cells,[9] but there is no substantial evidence on the lineages connecting oval cells and small hepatocytes.

Recently we identified AnxA3 as a small hepatocytes-specific protein,[17] and determined its expression profile in primary cultured hepatocytes.[17–19] AnxA3 was detected in primary cultures of hepatocytes at 48 h, but not in those cells at very beginning as early as 2.5 h, suggesting that AnxA3 is expressed by hepatocytes when they are reprimed to proliferate in culture. Any growth-promoting condition, *e.g.*, addition of epidermal growth factor (EGF) or hepatocyte growth factor (HGF)

† To whom correspondence should be addressed. Tel/Fax: +81-466-84-3949; E-mail: tseki@brs.nihon-u.ac.jp

Abbreviations: 2-AAF, 2-acetylaminofluoren; ALT, alanine amino transferase; AnxA3, annexin A3; AST, aspartic acid amino transferase; CCl_4, carbon tetrachloride; EGF, epidermal growth factor; HGF, hepatocyte growth factor; GAPDH, glyceraldehyde-3-phosphate dehydrogenase; siRNA, small-interfering RNA

to the culture medium, or inoculation of parenchymal cells with less population, enhances AnxA3 expression of hepatocytes. Conversely, suppression of AnxA3 gene expression with small-interfering RNA (siRNA) markedly inhibits growth of the transfected parenchymal hepatocytes.[18] As described above, we identified AnxA3 from isolated cultured small hepatocytes, and later we detected it in unfractionated hepatocytes cultured for 2 d. Thus the expression of AnxA3 might not be confined to small hepatocytes, and it might be implemented in cells that acquire growth potential or ones that recover dedifferentiating properties.[17]

Similar circumstances may occur *in vivo*, but little evidence has been obtained for the expression profile and pathophysiological role of AnxA3 in the liver *in vivo*. Hence we produced hepatic lesions in rats using 2-acetylaminofluoren/carbon tetrachloride (2-AAF/CCl_4), which is known to stimulate strongly the *in situ* emergence of hepatic progenitor cells, mainly ductular cells involving oval cells, in pericentral necrotic lesion and in periportal arborized ductular zones.[16,20]

In associating with hepatocyte damage in the pericentral area 2 d after 2-AAF/CCl_4 treatment, clustered cells expressed both AnxA3 and albumin emerge in the area, followed by disappearance of these cells and appearance of albumin/OV-6-positive oval cells. OV-6 is a specific marker for the oval cells.[21] Given the emergence of such unusual clusters, it is highly probable that the lesional reaction strongly elicited blood components including hematopoietic stem cells, macrophages and Kupffer cells, which closely relate to the emergence of clustered cells. The results of this investigation performed in an acute phase of liver failure failed to demonstrate the fate of AnxA3-positive cells. If these unusual cells have the potential to become mature hepatocytes, their differentiation is hampered in the presence of a hepatocyte-specific antimitotic agent, 2-AAF, so that one must discontinue this agent in order to determine the further fate of such cells. Since no one has demonstrated a substantial relationship between oval cells and small hepatocytes, we do not know yet whether the cells in clusters were progeny of oval cells. Hence we conclude that with agent-induced inflammation in the liver, AnxA3-positive cells emerge from the pericentral area, especially in the most necrotic zone, zone 3. Because these AnxA3-positive cells coexpressed albumin, they must have been a hepatocyte progenitor.

Materials and Methods

Induction of acute liver injury. All animal experiments were performed in accordance with the Guidelines for Animal Experiments of the College of Bioresource Sciences of Nihon University. Female F344 rats, 9 weeks old, purchased from Japan SLC (Shizuoka, Japan), were maintained on a standard diet, CE-2 (Clea Japan, Tokyo, Japan) and were allowed access to the diet and water freely. For the experimental onset of acute hepatic failure, rats were administered 2-AAF (Sigma-Aldrich, St. Louis, MO, USA) by oral gavage at a dose of 10 mg/kg body weight/d for up to 9 d. On the 5th day of 2-AAF administration, CCl_4 (Wako Pure Chemical Industries, Osaka, Japan) diluted 5 times with corn oil was given to rats as a bolus (CCl_4, 60 µl = 90 mg/100 g b.w., per os). Liver and blood samples were obtained from rats under anesthesia with Nembutal before and after treatment with CCl_4. To estimate the damage to the liver, serum levels of alanine amino transferase (ALT) and aspartic acid amino transferase (AST) were assayed using commercial kits (Wako).

RNA isolation and RT-PCR. Total RNA was extracted from the liver samples by the single-step method.[22] Real-time RT-PCR was performed with a rapid thermal cycler system, LightCycler (Roche Diganostics, Lewes, UK) as described elsewhere.[23] The primers for AnxA3 for PCR were as follows: 5′-CAA ATT CAC CGA GAT CCT GT-3′ and 5′-AGC AGC AGG TCT TCA AAA TG-3′. These primers were designed by referring to the gene sequences officially presented to the public by GenBank (AnxA3 = M012823), and synthesis was rendered to Nihon Gene Research Laboratories (Miyagi, Japan).

Immunohistochemical examination. Serial liver sections each cut 3 µm thick were prepared from paraformaldehyde-fixed paraffin-embedded blocks. The deparaffinated and rehydrated sections were heated for 5 min at 100 °C in 10 mM citrate buffer (pH 6.0), and treated with either 10% mouse serum (for counterstaining of albumin and AnxA3) or 10% bovine serum albumin (for other forms of staining) for 1 h. After they were washed with PBS, sections were incubated for 1 h with an specific antibody to each antigen. The antibodies used were anti-rat albumin goat IgG (MP Biomedicals, Aurora, OH, USA), diluted 1:800 before use, and anti-human AnxA3 rabbit IgG (1:200), a gift from Dr. F. Russo-Marie and Dr. C. Ragueness-Nicol. The fluorescence-labeled secondary antibodies were Cy3-labeld anti-goat murine IgG, 1:200 (Chemicon International, Temecula, CA, USA) and FITC-labeled anti-rabbit sheep IgG, 1:200 (MP Biomedicals). For observation of CD-34, tissue sections were incubated for 18 h at 4 °C with the primary antibody, anti-mouse CD34 rabbit IgG (1:200) (Santa Cruz Biotechnology, Santa Cruz, CA, USA), followed by incubation with secondary antibody, FITC-conjugated sheep anti-rabbit IgG, 1:100 (MP Biomedicals). To stain OV-6, deparaffinated sliced sections were incubated with primary monoclonal anti-human/rat OV-6 antibody (R&D Systems, Minneapolis, MN, USA), and treated with Histofine Simplestain Max PO (Nichirei, Tokyo, Japan). Then peroxidase activity on the secondary antibody was detected with 3,3′-diaminobenzidine (Merck, Tokyo, Japan).

Each liver section thus treated was mounted on a

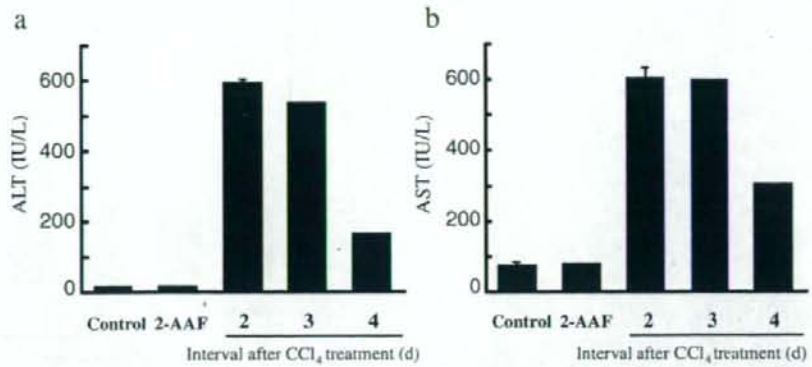

Fig. 1. Serum ALT and AST Activities of Normal Rats, and 2-AAF and 2-AAF/CCl_4-Treated Rats.

Serum ALT (a) and AST (b) activities were measured with commercial kits. There was no leakage of ALT or AST in rats treated with or without 2-AAF. However, CCl_4 treatment in the course of 2-AFF administration caused severe inflammation to the livers in several days, but, as shown by the ALT and AST values, these rats on the 4th day tended to recover from the inflammation. Bars represent the mean ± S.E. for 3 rats (control, 2-AAF, 2nd day), and the mean for 2 rats (3rd day and 4th day).

cover glass with a mounting medium, Vectashield (Vector Laboratories, Burlingame, CA, USA), and subjected to observation with a fluorescent microscope, Axioplan 2 (Carl Zeiss MicroImaging, Oberkochen, Germany).

Cryosection and Oil red O staining. Cryosections prepared from rat liver were stained with Oil red O and hematoxylin. Briefly, the liver tissues were fixed with paraformaldehyde and embedded in OCT compound (Sakura Finetek Japan, Tokyo, Japan), and then cut 8 μm thick to give serial sections. The tissue sections were dried by air, followed by immersion into 50% (v/v) aqueous isopropanol. Staining with a 60% Oil red O solution (Muto Pure Chemicals, Tokyo, Japan) was performed for 30 min at 37 °C, and sections were washed briefly with 50% aqueous isopropanol and distilled water. For morphologic observation of tissues and cellular nuclei, the sections were counterstained for 7 min with Mayer's hematoxylin (Wako). After they were washed with water, the sections were mounted with an aqueous mounting medium, Mount-Quick Aqueous (Daido Sangyo, Tokyo, Japan), and observed under a fluorescent microscope, Axioplan 2, with devised filter sets.

Results

Liver injury caused by 2-AAF/CCl_4

The rats treated by oral gavage of 2-AAF for 5 d did not show any marked increase in serum ALT or AST values (Fig. 1a and b), whereas, those that underwent a single treatment with CCl_4 and 2-AAF administration (the 2-AAF/CCl_4-treated rats) showed much higher levels of ALT and AST activities than untreated control or 2-AAF-treated alone. Each level of activity was highest in 2 d, and then decreased at 4 d after CCl_4 treatment. Thus our present protocol for intoxication of liver produced the acute hepatic lesions that healed to some extent within 4 d of injury; the recovery rate at this moment was estimated to be approximately 70% of the most serious lesion at 2 d in respect to the enzyme activities measured. The mode of ALT and AST elevation in our 2-AAF/CCl_4-treated rat model was quite similar to that of Sigala *et al.*,[24] although the maximum levels of ALT and AST in our model were 8 times and 3 times higher than those of Sigala *et al.*,[24] respectively, because we used CCl_4, 60 μl (approximately 90 mg)/100 g body weight, 1,000 more than that of Sigala *et al.*,[24] at 0.066 mg/100 g body weight.

The histological examination of the livers from 2-AAF/CCl_4-treated rats revealed that on the 2nd day after CCl_4 treatment there were large numbers of cell clusters stained densely with hematoxylin and eosin (H&E) in acinus zone 3 (Fig. 2a, arrowheads), the closest area to central vein (CV). In this area, there was also infiltration of inflammatory cells (Fig. 2a, thin arrows). Even the hepatocytes located in acinus zones 1 and 2 were abnormally distended by fat droplets (Fig. 2a, thick arrows, and b, Oil red O/hematoxylin stain).

On the 4th day after CCl_4 treatment, such steatotic livers with many clusters decreased markedly in number (Fig. 2c, Oil red O/hematoxylin stain), and necrotic image was alleviated in consistently with the restoration of chemical indications as shown in Fig. 1. The hepatocytes at this restored stage had microvesicular fat accumulation, if any fat accumulation (Fig. 2c, arrows).

Annexin A3 expression of intoxicated rat livers

The levels of AnxA3 mRNA expressed in the livers were measured quantitatively by RT-PCR. Since mRNA normalizers such as glyceraldehyde-3-phosphate dehy-

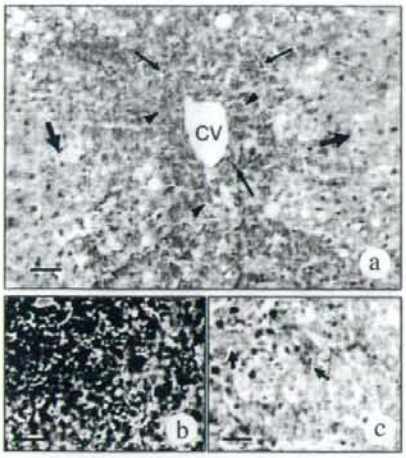

Fig. 2. Histological Examination of 2-AAF/CCl_4-Treated Rat Liver.
Inflammatory liver sections prepared from rats 2 d and 4 d after CCl_4 treatment were stained with H&E (a) or Oil red O/hematoxylin (b and c). In (a), H&E staining of the liver section showed characteristic red-colored clustered cells (arrowheads) immediately around the central vein (CV), corresponding to acinus zone 3. Surrounding these cells there were vacuoles, and on the outer boundary of the picture (a), distended hepatocytes with fat droplets can be seen (thick arrows). There were inflammatory cells in this area (thin arrows). As the lower panels show large fat droplets observed in the liver section at 2 d after 2-AAF/CCl_4 treatment (b) were mostly absorbed by hepatocytes (arrows in c). Scale bars = 50 μm.

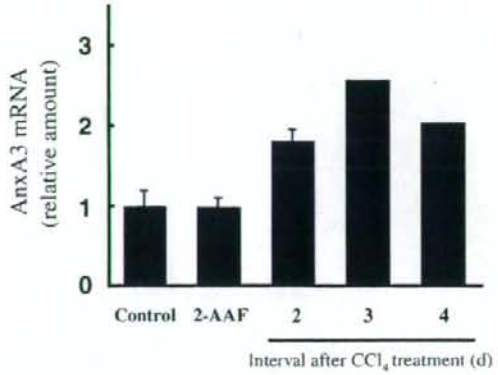

Fig. 3. AnxA3 Expression in 2-AAF/CCl_4-Treated Rat Livers.
Total liver RNA isolated was analyzed quantitatively by real-time PCR method using AnxA3-specific primers. Because of the heterogeneous expression of housekeeping genes, the data were not normalized with these genes. The ordinate shows the amounts of mRNA in the livers relative to that of control assumed to be 1.0. Bars represent the mean ± S.E. for three rats (control, 2AAF, 2nd d), and the mean for two rats (3rd d and 4th day).

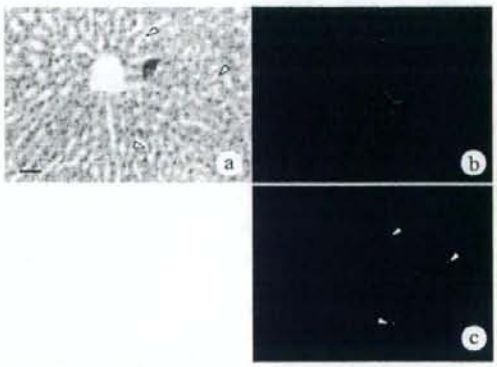

Fig. 4. Immunohistochemical Examination of AnxA3-Positive Cells in Normal Rat.
Serial liver sections prepared from normal control rats were stained with H&E (a), anti-rat albumin (b) and anti-human AnxA3 (c). The radial line up of hepatocyte architecture (a, H&E stain) was composed of albumin-producing parenchymal cells, as can be seen in the staining with anti-albumin/Cy3-antibodies (b). The AnxA3-producing nonparenchymal cells were slightly stained by anti-AnxA3/FITC-antibodies (arrowheads in c), and the positive cells can be seen on the H&E-stained section, apparently consistently with the forms of mononuclear cells (arrowheads in a). Scale bars = 50 μm.

drogenase (GAPDH) and β-actin were not constantly expressed in the livers of our 2-AAF/CCl_4-administered rat model as has been reported elsewhere,[25] the AnxA3 mRNA was normalized with total RNA extracted from the liver samples according to Bustin's recommendations.[25] Administration of 2-AAF alone to rats by oral gavage for 9–10 d hardly caused any change in their hepatic morphologies (data not shown). The AnxA3 mRNA levels of the livers from 2-AAF-treated rats were almost equal to those from control rats (Fig. 3), but in 2-AAF/CCl_4-treated rat livers, the AnxA3 levels were 2–2.5 times higher than those of untreated control rats (Fig. 3, see the bar at 3 d). The elevated level of AnxA3 lasted for 4 d after CCl_4 treatment, indicating that the AnxA3-positive cells are resistant to 2-AAF. A trace but certain level of AnxA3 mRNA in control rats (Fig. 3, left bar) can be explained by the presence of a small number of AnxA3-producing cells, which as described in Fig. 4 were determined histologically to be non-parenchymal cells in the liver.

The tissue section from the control rat liver (Fig. 4a, H&E stain) and its serial sections stained by fluorescence for albumin and AnxA3 (Fig. 4b and c) represent a typical hepatic cord with parenchymal cells expressing albumin (b). Although it was difficult to identify AnxA3-positive cells in the counterstained section, the fluorescence of AnxA3 disclosed that there was a trace population of AnxA3-positive cells (arrowheads in panel c), and these cells are determined to be mononuclear non-parenchymal cells (Fig. 4c, arrowheads indicate AnxA3-positive cells, and the serially prepared section-stained nuclei by H&E, Fig. 4a).

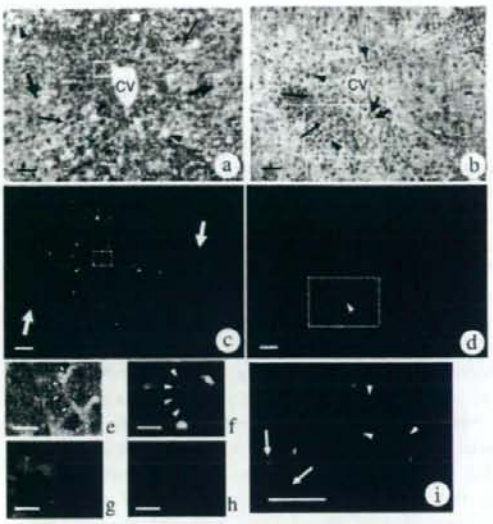

Fig. 5. Histological and Immunohistochemical Examinations of the Serially Prepared Liver Sections Prepared from 2-AAF/CCl_4-Treated Rats.

Figures 5a and b are H&E-stained sections of rat livers from 2 d (a) and 4 d (b) after CCl_4 treatment of rats, which had been administered 2-AAF by oral gavage for 5 d. Note the drastic changes caused around the pericentral region. One can see around the central vein (CV) newly formed clusters with a clear boundary between them (box in a), hepatocytes distended by lipid droplets (thick arrows), erythrocytes (thin arrows), and vacuoles formed after steatosis (arrowheads). The less-populated clusters remained at the lower left side of CV (b, thin arrows), with infiltrated inflammatory cells (arrowheads) and newly appearing ductular structures with many epithelial cells, indicating neo-angiogenetic reaction (thick arrows). Panels (c) and (d) are immunohistochemical observations of the serial liver sections from (a) and (b) respectively. A number of cells in the cluster were albumin as well as AnxA3-positive (c, see also higher magnitude e and f, in which the cells formed a cluster are encircled by arrowheads). The hepatocytes around the pericentral area were albumin-negative (arrows in c). Figure 5d and its higher magnitude (i) represent the appearance of oval cells in zone 2 in which oval cells strongly expressing albumin and the clusters expressing AnxA3 can be seen. Figure 5g shows CD34-positive cells in some places near CV in Fig. 5a. Figure 5h shows faintly-stained CD34 positive cells in some places in panel b. Scale bars in panels a–d and i = 50 μm; in panels e–h = 10 μm.

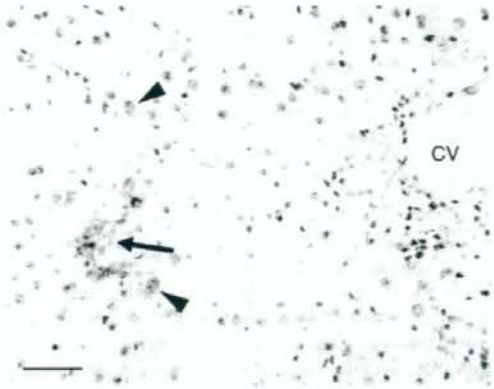

Fig. 6. The Occurrence of OV-6-Positive Cells in Zone2 4 Days after 2-AAF/CCl_4 Treatment.

OV-6-positive cells were localized either single (arrowheads) or in ductular form (arrow) around the CV, where clustering structures remained. Scale bar = 50 μm.

Appearance of annexin-positive and albumin-positive cells in the hepatic lesion

The serial sections prepared from the livers of 2-AAF/CCl_4-treated rats were subjected to immunohistochemical examination using antibodies specific to albumin and AnxA3 (Fig. 5). In H&E-stained sections, a striking drastic change in the rat liver was observed 2 d after CCl_4 treatment (Fig. 5a, see also Fig. 2a above). At this stage there were traces of necrosis with some bleeding in acinus zone 3 (Fig. 5a, thin arrows indicate erythrocytes among the clustered cells), and large numbers of clusters stained more clearly than other cells by hematoxylin were localized around the central vein (CV). The outer zone beyond the assembled line of vacuoles (Fig. 5a, arrowheads) was paved with hepatocytes, but these cells were abnormally extended by fat droplets to 30–40 μm diameter, and were closely attached each other (Fig. 5a, thick arrows).

Two days later, on the 4th day from 2-AAF/CCl_4-injury, the clusters were mostly replaced by a large number of epithelial-like cells with small nucleus and

Table 1. Summary of Changes in Cellular Phenotypes in Hepatic Lesions Caused by 2-AAF/CCl_4-Treatment

	Interval after CCl_4 treatment (d)								
	0			2			4		
Shape / Marker	●	●	●●	●	●	●●	●	●	●●
Annexin A3			−	+++		−	+/−	−	+/−
Albumin			++	+++		−	+/−	+++	+/−
CD34			−	+++		−	+/−	−	−
OV-6			−	−		−	−	+++	−

●. Clustered cells including blood corpuscle-like small cells; ●●. Hepatocytes; ●. Oval cells

Fluorescence intensity: −, not stained; +/−, faintly stained; +, weakly stained; ++, moderately stained; +++, strongly stained

The blank boxes under each cell shape represent absence of the cell type to be stained in the microscopic fields examined.

scant cytosol (Fig. 5b, thick arrows). Some clusters remaining at this stage can be seen in the box in Fig. 5b.

Immunohistochemical examination with fluorescence to albumin and AnxA3 was performed for identification of the cells emerging from the hepatic lesion. At 2 d after CCl_4 treatment, the pericentral region of the liver was stained positively with both fluorescences (Fig. 5c). The AnxA3-positive cells were localized in places where small cell-including clusters were present (Fig. 5a, H&E stain). The panels enlarged from the box in (c) make clear what cells were AnxA3-positive. One of the clusters (see the H&E-stained clusters in e, arrowheads) has a few fragments with fluorescence, and those might have been derived from different cells in the cluster. In addition, the yellow fluorescence shows that they merged with antigenicities of albumin and AnxA3 (f). The hepatocytes surrounding the pericentral area were not stained by fluorescence (c, white arrows).

On 4th day from 2-AAF/CCl_4 treatment, epithelial-like small cells appeared in the pericentral region (b, thick arrows), and these cells were determined to be immunologically negative to albumin and AnxA3 (Fig. 5d, serial section after b), but as shown in the boxed area in (d) and the magnified panel (i), there were oval cells with typical oval-shaped nuclei of albumin-positive immunologic phenotype in zone2 (h, arrowheads). The previously observed clusters that expressed albumin and AnxA3 at 2 d after treatment can be seen on the left side of the panel (i, arrows).

Figure 5g shows the presence of CD34-positive blood corpuscle-like cells among the clusters that appeared 2 d after 2-AAF/CCl_4-injury. Some of the albumin and AnxA3-positive clustered cells were also CD-34 positive cells.

As shown in Fig. 6, immunohistochemical examination of oval cells disclosed that these OV-6-positive cells existed in zone 2 either as a single cells (arrowheads) or as cells likely to form a ductular structure (arrow).

Our observations are summarized in Table 1. The liver intoxicated by the carcinogenic and inflammatory agents, 2-AAF/CCl_4, fell into acute liver failure in 2 d, and judged by chemical and histological analyses, it proceeded to the recovery stage 4 d after CCl_4 treatment. During the period of these 4 d, the cells that appeared or disappeared from the lesion changed strikingly. The clustered cells including several AnxA3 and albumin-positive small cells, which originated from blood corpuscle-like cells with CD34 antigen, appeared on day 2 and disappeared thereafter, and, in turn, oval cells emerged on day 4 from the ruins in zone 2 surrounding post-necrotic pericentral zone 3. The clustered cells and following oval cells are likely to have had independent progenies, since they emerged from different zones at different times. AnxA3 must be a protein expressed by the immature growing hepatocytes, which in this study did not differentiate further in the presence of 2-AAF.

Discussion

It is generally accepted that replication of lost cells or tissues of the liver can be done by the major hepatic residents, parenchymal hepatocytes, and that no other cells are required.[1,2,7,26,27] However, if proliferation of hepatocytes is blocked experimentally, bone marrow-derived hematopoietic stem cells, origin-unknown oval cells (stem-like cells) or proliferative small hepatocytes emerge from circulatory blood or from inside the liver.[4,5,28–32]

We identified AnxA3 as a protein expressed by smaller proliferative hepatocytes, that is, by cells with lower gravity, but not by differentiated mature parenchymal cells having higher gravity.[17] We also found that transfection of AnxA3-targeted siRNAs to primary cultured hepatocytes greatly suppressed DNA synthesis, and made DNA synthesis enhanced with either HGF or EGF invalid.[18] Thus we were able to demonstrate for the first time that AnxA3 plays a pivotal role in the multiplication of hepatocytes. Although the molecular function of hepatic AnxA3 is not yet known, it may be similar to that of microglia or neutorophils, in which AnxA3 works as a bridge to bind phospholipids and proteins, and granule to granule *via* Ca^{2+}.[33–36]

Hence study of growth-related AnxA3 in hepatocytes and related phenotypes, if any, during hepatic regeneration might help to determine how such cells acquire growth potential and differentiate into hepatocytes and hepatic ductular cells. To detect AnxA3 in an animal liver, we employed a 2-AAF/CCl_4-induced acute liver failure program, in which 2-AAF specifically inhibited hepatocyte mitosis and prevented cell proliferation and CCl_4 gave rise to hepatic injury through its reactive metabolite, trichloromethyl radical, generated in the first phase detoxification mechanism in hepatocytes.[37–39]

The combined use of these cytotoxic agents is known to cause hepatocyte damage specifically in the pericentral region, and strongly to stimulate restitution of the liver either by recruiting hematopoietic stem cells or by calling together endogenous cells, those which are 2-AAF resistant (primarily the oval-like cells).[9,40] Our present 2-AAF/CCl_4-injure program produced severe damage in pericentral zone3 2–3 d after treatment, and restored the lesion some 30% in 4 d (Fig. 1). In this model, the pericentral cellular phenotypes changed strikingly; *e.g.*, the typical hepatic cords made of albumin-producing hepatocytes with a trace population of AnxA3-positive non-parenchymal cells (Fig. 4) changed into severe lesions with newly appearing cell clusters including small hepatocyte-like cells. There was also infiltration of blood cells, erythrocytes and macrophages as well as the bone marrow-derived hematopoietic cells as has been demonstrated by Yin, *et al.*[39] (Figs. 2 and 5). Immunohistochemical examination showed that some of the cells in a cluster coexpressed AnxA3 and albumin, and also expressed CD34 (Fig. 5). Therefore, some of these cells appeared to have been

derived from the bone marrow, and then committed to become hepatocytes. For this commitment, several factors are required, *e.g.*, a serum factor occurring in rodents with severe liver damage.[41]

In respect to the striking changes in cellular phenotypes observed in the lesion, it is most plausible to think that in our animal model the damaged hepatocytes with 2-AAF/CCl_4 were replaced by agent-resistant hematopoietic stem cells, and that, receiving strong stimulative pressure for restitution, these new dwellers had to form a cluster to live under the agent (2-AAF)-induced antiproliferative condition. Nevertheless, they broke up the cluster in 2 d, for the following reasons: i) the AnxA3-positive cells did not become mature hepatocytes, because hepatocytes are 2-AAF-susceptible and ii) the AnxA3-positive cells do not have sufficient longevity to live longer, so that they were scavenged by macrophages or Kupffer cells or disappeared by apoptosis. As has been reported by many investigators, oval cells scattered around the central vein (Figs. 5h and 6) can differentiate further into hepatocytes *via* the massive emergence of small hepatocytes, if 2-AAF is withdrawn from the animal.[39,42–44]

In the present study, we observed under pathological conditions with 2-AAF/CCl_4-injury a striking change in cellular phenotypes that might work for rebuilding of the damaged liver, because the rats remaining without sacrifice were able to survive. This is the first report of the appearance of AnxA3-expressing small cell clusters in an acute hepatic lesion. Since AnxA3 is expressed when hepatocytes acquire growth potential,[17] its expression by cells coexpressed with albumin in hepatic lesions should be a trigger for parenchymal cell generation. The fate of AnxA3-producing cells in relation to the restitution of the entire liver involving periportal zone1 remains to be elucidated.

Acknowledgments

We thank Mr. Yuta Ogawa for technical assistance. This work was supported by grants from the following sources: (i) For Health Science Research from the Japanese Ministry of Health, Labor and Welfare (to S.N.), (ii) Academic Frontier Project (to T.S.) from the Ministry of Education, Culture, Sports, Science, and Technology of Japan. Y.I. was supported by a Fellowship from the Academic Frontier Project.

References

1) Fabrikant, J. I., Studies on cell population kinetics in the regenerating liver. *Natl. Cancer Inst. Monogr.*, **30**, 169–183 (1969).
2) Michalopoulos, G. K., and DeFrances, M. C., Liver regeneration. *Science*, **276**, 60–66 (1997).
3) Parent, R., Marion, M. J., Furio, L., Trepo, C., and Petit, M. A., Origin and characterization of a human bipotent liver progenitor cell line. *Gastroenterology*, **126**, 1147–1156 (2004).
4) Vig, P., Russo, F. P., Edwards, R. J., Tadrous, P. J., Wright, N. A., Thomas, H. C., Alison, M. R., and Forbes, S. J., The sources of parenchymal regeneration after chronic hepatocellular liver injury in mice. *Hepatology*, **43**, 316–324 (2006).
5) Yavorkovsky, L., Lai, E., Ilic, Z., and Sell, S., Participation of small intraportal stem cells in the restitutive response of the liver to periportal necrosis induced by allyl alcohol. *Hepatology*, **21**, 1702–1712 (1995).
6) Lagasse, E., Connors, H., Al-Dhalimy, M., Reitsma, M., Dohse, M., Osborne, L., Wang, X., Finegold, M., Weissman, I. L., and Grompe, M., Purified hematopoietic stem cells can differentiate into hepatocytes *in vivo*. *Nat. Med.*, **6**, 1229–1234 (2000).
7) Dabeva, M. D., Alpini, G., Hurston, E., and Shafritz, D. A., Models for hepatic progenitor cell activation. *Proc. Soc. Exp. Biol. Med.*, **204**, 242–252 (1993).
8) Theise, N. D., Saxena, R., Portmann, B. C., Thung, S. N., Yee, H., Chiriboga, L., Kumar, A., and Crawford, J. M., The canals of Hering and hepatic stem cells in humans. *Hepatology*, **30**, 1425–1433 (1999).
9) Lemire, J. M., Shiojiri, N., and Fausto, N., Oval cell proliferation and the origin of small hepatocytes in liver injury induced by D-galactosamine. *Am. J. Pathol.*, **139**, 535–552 (1991).
10) Alison, M., Golding, M., Lalani, E. N., Nagy, P., Thorgeirsson, S., and Sarraf, C., Wholesale hepatocytic differentiation in the rat from ductular oval cells, the progeny of biliary stem cells. *J. Hepatol.*, **26**, 343–352 (1997).
11) Sirica, A. E., and Williams, T. W., Appearance of ductular hepatocytes in rat liver after bile duct ligation and subsequent zone 3 necrosis by carbon tetrachloride. *Am. J. Pathol.*, **140**, 129–136 (1992).
12) Tateno, C., Takai-Kajihara, K., Yamasaki, C., Sato, H., and Yoshizato, K., Heterogeneity of growth potential of adult rat hepatocytes *in vitro*. *Hepatology*, **31**, 65–74 (2000).
13) Sidler Pfandler, M. A., Hochli, M., Inderbitzin, D., Meier, P. J., and Stieger, B., Small hepatocytes in culture develop polarized transporter expression and differentiation. *J. Cell Sci.*, **117**, 4077–4087 (2004).
14) Herrera, M. B., Bruno, S., Buttiglieri, S., Tetta, C., Gatti, S., Deregibus, M. C., Bussolati, B., and Camussi, G., Isolation and characterization of a stem cell population from adult human liver. *Stem Cells*, **24**, 2840–2850 (2006).
15) Avril, A., Pichard, V., Bralet, M. P., and Ferry, N., Mature hepatocytes are the source of small hepatocyte-like progenitor cells in the retrorsine model of liver injury. *J. Hepatol.*, **41**, 737–743 (2004).
16) Best, D. H., and Coleman, W. B., Treatment with 2-AAF blocks the small hepatocyte-like progenitor cell response in retrorsine-exposed rats. *J. Hepatol.*, **46**, 1055–1063 (2007).
17) Niimi, S., Oshizawa, T., Yamaguchi, T., Harashima, M., Seki, T., Ariga, T., Kawanishi, T., and Hayakawa, T., Specific expression of annexin III in rat small hepatocytes. *Biochem. Biophys. Res. Commun.*, **300**, 770–774 (2003).
18) Niimi, S., Harashima, M., Gamou, M., Hyuga, M., Seki,

T., Ariga, T., Kawanishi, T., and Hayakawa, T., Expression of annexin A3 in primary cultured parenchymal rat hepatocytes and inhibition of DNA synthesis by suppression of annexin A3 expression using RNA interference. *Biol. Pharm. Bull.*, **28**, 424–428 (2005).

19) Harashima, M., Niimi, S., Koyanagi, H., Hyuga, M., Noma, S., Seki, T., Ariga, T., Kawanishi, T., and Hayakawa, T., Change in annexin A3 expression by regulatory factors of hepatocyte growth in primary cultured rat hepatocytes. *Biol. Pharm. Bull.*, **29**, 1339–1343 (2006).

20) Alison, M. R., Poulsom, R., Jeffery, R., Dhillon, A. P., Quaglia, A., Jacob, J., Novelli, M., Prentice, G., Williamson, J., and Wright, N. A., Hepatocytes from non-hepatic adult stem cells. *Nature*, **406**, 257 (2000).

21) Dunsford, H. A., and Sell, S., Production of monoclonal antibodies to preneoplastic liver cell populations induced by chemical carcinogens in rats and to transplantable Morris hepatomas. *Cancer Res.*, **49**, 4887–4893 (1989).

22) Chomczynski, P., and Sacchi, N., Single-step method of RNA isolation by acid guanidinium thiocyanate-phenol-chloroform extraction. *Anal. Biochem.*, **162**, 156–159 (1987).

23) Heid, C. A., Stevens, J., Livak, K. J., and Williams, P. M., Real time quantitative PCR. *Genome Res.*, **6**, 986–994 (1996).

24) Sigala, F., Kostopanagiotou, G., Andreadou, I., Kavatzas, N., Felekouras, E., Sigalas, P., Bastounis, E., and Papalambros, E., Histological and lipid peroxidation changes after administration of 2-acetylaminofluorene in a rat liver injury model following selective periportal and pericentral damage. *Toxicology*, **196**, 155–163 (2004).

25) Bustin, S. A., Quantification of mRNA using real-time reverse transcription PCR (RT-PCR): trends and problems. *J. Mol. Endocrinol.*, **29**, 23–39 (2002).

26) Coleman, J. P., Kirby, L. C., Setchell, K. D., Hylemon, P. B., Pandak, M., Heuman, D. M., and Vlahcevic, Z. R., Metabolic fate and hepatocyte toxicity of reverse amide analogs of conjugated ursodeoxycholate in the rat. *J. Steroid Biochem. Mol. Biol.*, **64**, 91–101 (1998).

27) Koch, K. S., and Leffert, H. L., Normal liver progenitor cells in culture. In "Stem Cells Handbook," ed. Sell, S., Humana Press, Totowa, pp. 367–384 (2004).

28) Mitaka, T., Hepatic stem cells: from bone marrow cells to hepatocytes. *Biochem. Biophys. Res. Commun.*, **281**, 1–5 (2001).

29) Thorgeirsson, S. S., and Grisham, J. W., Overview of recent experimental studies on liver stem cells. *Semin. Liver Dis.*, **23**, 303–312 (2003).

30) Menthena, A., Deb, N., Oertel, M., Grozdanov, P. N., Sandhu, J., Shah, S., Guha, C., Shafritz, D. A., and Dabeva, M. D., Bone marrow progenitors are not the source of expanding oval cells in injured liver. *Stem Cells*, **22**, 1049–1061 (2004).

31) Gleiberman, A. S., Encinas, J. M., Mignone, J. L., Michurina, T., Rosenfeld, M. G., and Enikolopov, G., Expression of nestin-green fluorescent protein transgene marks oval cells in the adult liver. *Dev. Dyn.*, **234**, 413–421 (2005).

32) Ong, S. Y., Dai, H., and Leong, K. W., Inducing hepatic differentiation of human mesenchymal stem cells in pellet culture. *Biomaterials*, **27**, 4087–4097 (2006).

33) Konishi, H., Namikawa, K., and Kiyama, H., Annexin III implicated in the microglial response to motor nerve injury. *Glia*, **53**, 723–732 (2006).

34) Le Cabec, V., and Maridonneau-Parini, I., Annexin 3 is associated with cytoplasmic granules in neutrophils and monocytes and translocates to the plasma membrane in activated cells. *Biochem. J.*, **303**, 481–487 (1994).

35) Sopkova, J., Raguenes-Nicol, C., Vincent, M., Chevalier, A., Lewit-Bentley, A., Russo-Marie, F., and Gallay, J., Ca(2+) and membrane binding to annexin 3 modulate the structure and dynamics of its N terminus and domain III. *Protein Sci.*, **11**, 1613–1625 (2002).

36) Rosales, J. L., and Ernst, J. D., Calcium-dependent neutrophil secretion: characterization and regulation by annexins. *J. Immunol.*, **159**, 6195–6202 (1997).

37) Gordis, E., Lipid metabolites of carbon tetrachloride. *J. Clin. Invest.*, **48**, 203–209 (1969).

38) Petersen, B. E., Goff, J. P., Greenberger, J. S., and Michalopoulos, G. K., Hepatic oval cells express the hematopoietic stem cell marker Thy-1 in the rat. *Hepatology*, **27**, 433–445 (1998).

39) Yin, L., Lynch, D., Ilic, Z., and Sell, S., Proliferation and differentiation of ductular progenitor cells and littoral cells during the regeneration of the rat liver to CCl_4/2-AAF injury. *Histol. Histopathol.*, **17**, 65–81 (2002).

40) Sell, S., Osborn, K., and Leffert, H. L., Autoradiography of "oval cells" appearing rapidly in the livers of rats fed N-2-fluorenylacetamide in a choline devoid diet. *Carcinogenesis*, **2**, 7–14 (1981).

41) Hong, H., Chen, J. Z., Zhou, F., Xue, L., and Zhao, G. Q., Influence of serum from liver-damaged rats on differentiation tendency of bone marrow-derived stem cells. *World J. Gastroenterol.*, **10**, 2250–2253 (2004).

42) Yoon, B. I., Choi, Y. K., and Kim, D. Y., Differentiation processes of oval cells into hepatocytes: proposals based on morphological and phenotypical traits in carcinogen-treated hamster liver. *J. Comp. Pathol.*, **131**, 1–9 (2004).

43) Bustos, M., Sangro, B., Alzuguren, P., Gil, A. G., Ruiz, J., Beraza, N., Qian, C., Garcia-Pardo, A., and Prieto, J., Liver damage using suicide genes. A model for oval cell activation. *Am. J. Pathol.*, **157**, 549–559 (2000).

44) Crosby, H. A., Hubscher, S., Fabris, L., Joplin, R., Sell, S., Kelly, D., and Strain, A. J., Immunolocalization of putative human liver progenitor cells in livers from patients with end-stage primary biliary cirrhosis and sclerosing cholangitis using the monoclonal antibody OV-6. *Am. J. Pathol.*, **152**, 771–779 (1998).

An inter-laboratory study to validate quantitative and qualitative immunoassay kits for screening test of aflatoxin B_1 in corn

Yoshiko SUGITA-KONISHI[1], Shingo NIIMI[2] and Kei-ichi SUGIYAMA[1]

[1] Division of Microbiology, National Institute of Health Sciences
(1-18-1, Kamiyoga, Setagaya-ku, Tokyo 158-8501, Japan)
[2] Division of Biological Chemistry and Biologicals, National Institute of Health Sciences
(1-18-1, Kamiyoga, Setagaya-ku, Tokyo 158-8501, Japan)

Collaborators: Eiichi ISHIKURO[3], Toshitsugu TANAKA[4], Yoshitsugu SUGIURA[4], Yoshinori ITOH[5] and Masahiro NAKAJIMA[6]

[3] The Fertilizer and Feed Inspection Service
(2-1, Shinntoshin, Chuo-ku, Saitama, 330-9733, Japan)
[4] Kobe Institute of Health
(4-6 Minatojima-Nakamachi, Chuo-ku, Kobe, Hyogo 650-0046, Japan)
[5] Division of Biomedical Food Research, National Institute of Health Sciences
(1-18-1, Kamiyoga, Setagaya-ku, Tokyo 158-8501, Japan)
[6] Nagoya city Public Health Research Institute
(1-11, Hagiyama, Mizuho-ku, Nagaya 467-8615, Japan)

Summary

To validate commercial kit for screening of the presence of AFB_1 in corn, an inter-laboratory study was conducted to evaluate three quantitative and two qualitative immunoassay kits designed for the detection of aflatoxins. Four laboratories performed a screen for the presence of aflatoxin B_1 (AFB_1) in corn. As for the quantitative kits, repeatability relative standard deviation (RSD_r) and reproducibility relative standard deviation (RSD_R) were estimated. One laboratory evaluated the lot variation of each quantitative kit. All kits used in this study showed that the RSD_r and RSD_R were less than 23.3 % and 35.7 %, respectively, in spiked or naturally contaminated corn samples. As for the qualitative kits, neither false positive nor false negative results were found in corn samples (blank, spiked or naturally contaminated samples) in any laboratories. The RSDs in the lot variation of the same quantitative kit was less than 46.5 % in both two brands. The results appeared to indicate that all kits tested in this study could be validated for the screening of the presence of AFB_1 in corn, and were also available for the first step of the detection of AFB_1 at levels of more than 5 ng/g.

Key words : inter-laboratory study, immunoassay kit, aflatoxin, corn

(Received: January 15, 2007, Accepted: April 23, 2007)

Introduction

Aflatoxins (AFs: Aflatoxin B_1, B_2, G_1 and G_2) produced by *Aspergillus flavus* and *A. parasiticus* are well-known as carcinogenic mycotoxins. Especially, Aflatoxin B_1 (AFB_1) is the most frequently encountered among AFs and possesses a high toxic potential[1] responsible for human liver cancer. The contamination of AFs has been found in corn, beans, peanut, tree nuts as well as in animal feed[2].

Many analytical methods have been conducted to detect AFs in foods and feeds[3,4], however, most of them require sophisticated equipment and are time-consuming. Recently commercially available immunoassay kits were introduced for the detection of AFs. These assays are timesaving and do not use expensive instruments. The positive and negative results can be visualized directly or measured by a micro-well reader. These rapid analytical immunoassay kits for mycotoxins have been supplied from several chemical companies, and it is convenience to detect the target easily. The commercial kits are divided into two analytical types. One is a quantitative determination such as enzyme-linked immunosorbent assay (ELISA) and quantitative lateral flow test. The other is a qualitative rapid detection such as rapid membrane-based enzyme immunoassay.

To estimate the efficiency of commercial immunoassay kits in screening of corn containing AFB_1 exceed the regulatory limit, we carried out four inter-laboratory studies using blank, spiked, and naturally contaminated corn. Additionally, the variation of lots in the same kit was carried out by one of the participating laboratories. Using the same samples, the assays were performed in triplicate in each lot of the kit.

Materials and Methods

Immunoassay kits Table 1 summarizes the specification of 5 commercial kits for this study with target chemicals and detectable ranges. The kits A, C and E are for total aflatoxins, while kits B and D are only for AFB_1. As commercial kits, Agra Quant Total Aflatoxin Assay 4/40 (Romer Lab.), ROSA Aflatoxin quantitative (Charm Sciences inc.), RIDASCREEN FAST aflatoxin (R-biopharm Rhone Ltd.), AFLACARD B_1 (R-biopharm Rhone Ltd., 4 ng/g Cut-off.) and AgraStrip™ Total Aflatoxin Test (Romer Lab., 4 ng/g Cut-off) were used. Due to the Food Sanitation Law of Japan that defines the guideline to regulate only AFB_1 in all foods, AFB_1 was used as a spiked aflatoxin into analytical samples throughout this inter-laboratory study.

Table 1. The specification of the kit tested in the inter-laboratory study

Kit	Quantitative/qualitative	Range for detection (ng/g)	Target for detection
Kit A	quantitavtive (ELISA)	1 ~ 20	total aflatoxin
Kit B	quantitavtive (ELISA)	0 ~ 45	aflatoxin B_1
Kit C	quantitavtive (lateral-flow)	0 ~ 100	total aflatoxin
Kit D	qualitative	> 4	aflatoxin B_1
Kit E	qualitative	> 4	total aflatoxin

Sample preparation and test procedure Blank corn kernels, which contained less than 1 ng/g of AFs, were obtained from the Fertilizer and Feed Inspection Service, Japan. The corn kernels were ground in a grinder to a mesh size of 1 mm. Two spiked samples were prepared by adding an appropriate volume of AFB_1 (1 μg/ml) dissolved in acetonitrile to 10 g of blank material. Final concentrations of AFB_1 were adjusted to 5 ng/g and 10 ng/g. Natural contaminated corn containing 10.7 ± 2.2 ng/g of AFB_1 alone was purchased from R-biopharm Rhone Ltd. as a standard material.

Sample extraction and test procedures were carried out according to the manufacturer's instruction in each kit.

Inter-laboratory study This study has been performed by four laboratories, National Institute of Health Sciences (division of microbiology, division of biological chemistry and biologicals, and division of biomedical food research), Kobe Institute of Health, Nagoya city Public Health Research Institute and Japan Food Research Laboratories. National Institute of Health Sciences (division of microbiology and division of biological chemistry and biologicals) conducted the study containing preparation of all samples and protocols and others were participants. Kits and samples (blank or naturally contaminated corn) were stored at 2-8 ℃ after being received. Test samples were measured with their own micro-well reader at suitable wavelength in the quantitative assay, and the interpretation of the results was visually determined in the qualitative assay. In these experiments, duplicate analyses were performed for each kit.

Statistics Parameters of precision, which are the inter-laboratory means, RSDr, RSD_R, were deduced using an analysis of variances according to the AOAC guideline[5].

Results and Discussion

The aim of this study was to evaluate whether these kits are suitable for the screening of AFB_1-contaminated corn at levels of more than 10 ng/g. Taking account the unexpected errors in the steps of extraction and analytical practice, the cut-off value of the results was set at around 5 ng/g. Therefore in all kits validated in this study, the range for detection covered 5 ng/g.

In Table 2-1, the RSD_r of two quantitative kits (A and B) showed that the RSD_r was 12.7 and 16.6 % for 5 ng/g of AFB_1 spiked sample, 6.2 and 7.4 % for 10 ng/g spiked, and 4.8 and 16.4 % for naturally contaminated samples, respectively, while the RSD_R of kit A and kit B were 20.5 and 20.0 %, 14.6 and 14.5 %, and 13.3 and 30.6 %, respectively. The correlation coefficients of kits A and B in four laboratories were 0.982-1.0 and 0.995-0.996, respectively. Kit C, which is a quantitative lamina flow kit, showed that RSD_r and RSD_R were less than 23.3 % and 35.7 %, respectively. The data indicated that the RSD_r and RSD_R values of kit C were higher than those of kits A and B. In the qualitative kits, shown in Table 2-2, kits D and E showed neither false positive in blank corn nor false negative in spiked or naturally contaminated samples. The results obtained here demonstrated that the quantitative and qualitative kits tested in this study were successfully utilized for the detection of AFB_1 in aflatoxin-contaminated corn.

In Table 3, the results of the variation between different lots of the same kit are shown. The RSD between lots of the kit A was 11.4 % for the spiked corn with 5 ng/g AFB_1, 3.5 % for the spiked corn with 10 ng/g AFB_1, and 10.9 % for naturally contaminated corn. In kit C of the lateral flow method, the

Table 2-1. Interlaboratory study results for determination of AFB_1 in corn by immunoassay tests (Quantitative kit)

	Laboratory No.	Laboratory 1		Laboratory 2		Laboraty 3		Laboratory 4		Results		
	Number of test	test 1 (ng/g)	test 2 (ng/g)	test 1 (ng/g)	test 2 (ng/g)	test 1 (ng/g)	test 2 (ng/g)	test 1 (ng/g)	test 2 (ng/g)	Mean (ng/g)	RSDr (%)	RSD_R (%)
Kit A	Blank	ND	ND	ND	ND	ND	ND	ND	ND	–	–	–
	5 ng/g spike	2.2	3.4	4.4	4.5	4.3	3.8	3.8	3.5	3.7	12.7	20.5
	10 ng/g spike	7.5	7.5	8.4	9.0	7.9	7.3	6.7	5.7	7.5	6.2	14.6
	naturally contamination	8.9	8.2	7.1	7.4	9.2	8.7	7.1	6.6	7.9	4.8	13.3
Kit B	Blank	ND	ND	ND	ND	1.78	1.78	ND	ND	–	–	–
	5 ng/g spike	5.0	5.5	4.1	4.8	4.5	5.7	2.9	4.4	4.6	16.6	20.0
	10 ng/g spike	8.0	7.5	7.0	8.1	9.5	8.7	6.3	6.8	7.7	7.7	14.5
	naturally contaminated	8.3	7.6	3.7	7.5	11.3	11.6	9.2	8.5	8.5	16.4	30.6
Kit C	Blank	1	1	1	1	ND	ND	1	1	–	–	–
	5 ng/g spike	8	5	3	4	4	4	5	6	4.5	23.3	38
	10 ng/g spike	19	12	7	13	14	11	8	12	11.2	2.7	31.2
	naturally contaminated	12	15	5	15	10	9	7	8	9	12.2	35.7

ND: Not determined
RSDr: repeatability relative standard deviation
RSD_R: reproducibility relative standard deviation

Table 2-2. Interlaboratory study results for determination of AFB_1 in corn by immunoassay tests (Qualitative kit)

	Laboratory No.	Laboratory 1		Laboratory 2		Laboraty 3		Laboratory 4	
	Number of test	test 1 (ng/g)	test 2 (ng/g)	test 1 (ng/g)	test 2 (ng/g)	test 1 (ng/g)	test 2 (ng/g)	test 1 (ng/g)	test 2 (ng/g)
Kit D	Blank	–	–	–	–	–	–	–	–
	5 ng/g spike	+	+	+	+	+	+	+	+
	10 ng/g spike	+	+	+	+	+	+	+	+
	naturally contaminated	+	+	+	+	+	+	+	+
Kit E	Blank	–	–	–	–	–	–	–	–
	5 ng/g spike	+	+	+	+	+	+	+	+
	10 ng/g spike	+	+	+	+	+	+	+	+
	naturally contaminated	+	+	+	+	+	+	+	+

ND: Not determined
RSDr: repeatability relative standard deviation
RSD_R: reproducibility relative standard deviation

RSD of corns spiked with 5 ng/g, 10 ng/g, and naturally contaminated corn was 24 %, 46.5 %, and 4.4 %, respectively. In the kits D and E, no positive result appeared in blank sample and no negative result was recognized in corn spiked with 5 ng/g, 10 ng/g or naturally contaminated (data not shown). As for kit B, the manufacturing company supplies only one lot for this study.

In the quantitative assay, the results suggested that kits A and B were more robust than kit C, but they needed a more complicate procedure than kit C. Taking the performance of these kits into account, the users have to choose a kit which is suitable for their own purpose.

Taken together, 5 commercially available immunoassay kits were subjected to an inter-laboratory study involving 4 participants, and the results obtained in the present study validated the accuracy and reproducibility of the quantitative kits for AFB_1 in corn, showing that all kits are also able to screen the presence of AFB_1 in corn.

Table 3. The lot variation of quantitative kits

Kit	Sample	Mean (ng/g)	RSD (%)
Kit A	Blank	–	–
	5 ng/g spike	4.1	11.4
	10 ng/g spike	7.9	3.5
	naturally contaminated	9.5	10.9
Kit C	Blank	–	–
	5 ng/g spike	5.5	24.1
	10 ng/g spike	15.0	46.5
	naturally contaminated	8.8	4.4

RSD: relative standard deviation

References

1) IARC: "IARC monographs on the evaluation of carcinogenic risks to humans", pp. 245-395 (1993), World Health Organization /Intaernational Agency for Research on Cancer, Lyon.

2) JECFA: Aflatoxins, WHO Food Additives Series, **40**, pp. 359-468, (1998). World Health Organization, Geneva, Switzeland.

3) Jaimez, J., Fente, C.A., Vazquez, B.I., Franco, C.M., Cepeda, A., Mahuzier, G., Prognon, P.: J. Chromatogr. A, **882**, 1-10 (2000)

4) Scott, P.M.: Food Addit. Contam., **12**, 395-403 (1995)

5) Youden, W.J., Steiner, E.H.: "Statistical analysis" (eds. Youden, W.J., Steiner E.H.), pp. 72-83 (1975), Association of Official Analytical Chemists, Arlington, USA.

複数試験機関によるトウモロコシ中のアフラトキシン B_1 を検出する簡易測定法キットの妥当性試験

小西（杉田）良子，新見伸吾，杉山圭一：国立医薬品食品衛生研究所（158-8501　東京都世田谷区上用賀 1-18-1）
コラボレーター：
石黒瑛一：独立行政法人肥飼料検査所（330-9733　さいたま市中央区新都心 2-1）
田中敏嗣，杉浦義紹：神戸市環境保健研究所（650-0046　神戸市中央区港島中町 4-6）
中島正博：名古屋市衛生研究所（467-8615　名古屋市瑞穂区萩山町 1-11）
伊藤嘉典：国立医薬品食品衛生研究所（158-8501　東京都世田谷区上用賀 1-18-1）

トウモロコシ中のアフラトキシン B_1 を簡易迅速に測定できる市販のキットに関して，その妥当性を複数試験機関により評価した．市販のキットから，3 種類の定量用キット，2 種類の定性用キットを選定し妥当性試験に供した．対象試料としては，ブランクのトウモロコシおよび自然汚染トウモロコシを用いた．ブランクのトウモロコシは，添加回収試験（5 ng/g および 10 ng/g）に供した．定量性キットとして，ELISA 法とラテラルフロー法を試験対象として行った．これらの RSD_r は 23.3 %以下，RSD_R は 35.7 %以下であった．定性用キットにおいては，5 ng/g のアフラトキシン B_1 を添加したトウモロコシ，自然汚染のトウモロコシから擬陰性反応は見られず，ブランク試料から擬陽性は認められなかった．

同一キット中のロット間の変動性においては，ラテラルフロー定量法は ELISA 定量法より比較的高い傾向があり，妥当性試験の結果と同様，擬陽性または擬陰性の反応は認められなかった．

以上のことから，試験対象をトウモロコシに限れば，日本のアフラトキシン B_1 の規制検査において，5 ng/g を限度とした初期段階に用いるスクリーニング法として，これらの 5 種類のキットは，妥当であることが評価された．

キーワード：室間共同試験，イムノアッセイキット，アフラトキシン，トウモロコシ

THE JOURNAL OF BIOLOGICAL CHEMISTRY VOL. 282, NO. 46, pp. 33507–33514, November 16, 2007

A New Role of Thrombopoietin Enhancing *ex Vivo* Expansion of Endothelial Precursor Cells Derived from AC133-positive Cells*

Received for publication, May 14, 2007, and in revised form, September 5, 2007 Published, JBC Papers in Press, September 7, 2007, DOI 10.1074/jbc.M703919200

Toshie Kanayasu-Toyoda[‡], Akiko Ishii-Watabe[‡], Takayoshi Suzuki[§], Tadashi Oshizawa[§], and Teruhide Yamaguchi[‡1]

From the Divisions of [‡]Biological Chemistry and Biologicals, and [§]Cellular and Gene Therapy Products, National Institute of Health Sciences, Kamiyoga 1-18-1, Setagayaku, Tokyo 158-8501, Japan

We previously reported that CD31^{bright} cells, which were sorted from cultured AC133$^+$ cells of adult peripheral blood cells, differentiated more efficiently into endothelial cells than CD31$^+$ cells or CD31$^-$ cells, suggesting that CD31^{bright} cells may be endothelial precursor cells. In this study, we found that CD31^{bright} cells have a strong ability to release cytokines. The mixture of vascular endothelial growth factor (VEGF), thrombopoietin (TPO), and stem cell factor stimulated *ex vivo* expansion of the total cell number from cultured AC133$^+$ cells of adult peripheral blood cells and cord blood cells, resulting in incrementation of the adhesion cells, in which endothelial nitric oxide synthase and kinase insert domain-containing receptor were positive. Moreover, the mixture of VEGF and TPO increased the CD31^{bright} cell population when compared with VEGF alone or the mixture of VEGF and stem cell factor. These data suggest that TPO is an important growth factor that can promote endothelial precursor cells expansion *ex vivo*.

Neovascularization is an important adaptation to rescue tissue from critical ischemia. Postnatal blood vessel formation was formerly thought to be primarily due to the migration and proliferation of preexisting, fully differentiated endothelial cells, a process referred to as angiogenesis. Recent studies provide increasing evidence that circulating bone marrow-derived endothelial progenitor cells (EPCs)[2] contribute substantially to adult blood vessel formation (1–5). Cell therapy using EPCs is widely performed to rescue tissue damaged due to critical ischemia.

Although EPCs have been thought to be derived from many kinds of cells, cells characterized as CD34$^+$ (6), AC133$^+$ (7, 8), and CD14$^+$ (9) are also thought to differentiate to EPCs. The main role of EPCs has been thought to be the release of angiogenic factors such as interleukin-8 (IL-8), granulocyte colony-stimulating factor (G-CSF), hepatocyte growth factor, and vascular endothelial growth factor (VEGF) (9). To obtain a sufficient number of EPCs for the treatment may be very important in cell therapy for critical ischemia.

On the other hand, EPCs are mobilized from bone marrow by many substances such as G-CSF (10), granulocyte macrophage-colony stimulating factor (GM-CSF) (5), VEGF (3), erythropoietin (11–13), and statins (14, 15) *in vivo*. To get as many EPCs as possible without unduly burdening the patient, it is desirable to establish efficient expansion methods for EPCs *in vitro*.

Thrombopoietin (TPO), initially identified as the primary regulator of platelet production (16), plays an important and nonredundant role in the self-renewal of and expansion methods for hematopoietic stem cells (17–19). Recently, TPO has been found to exert a proangiogenic effect on cultured endothelial cells (20). The mechanism by which hematopoietic cytokines support revascularization *in vivo*, however, remains unknown. TPO has increased the number of colony-forming units-granulocyte-macrophage (21) and of burst-forming units-erythroid (22) *in vivo* and leads to a redistribution of colony-forming units-erythroid from marrow to spleen. Moreover, TPO acts in synergy with erythropoietin to increase the growth of burst-forming units-erythroid and the generation of colony-forming units-erythroid from marrow cells (21, 23, 24).

In our previous study (25), we isolated AC133$^+$ cells and examined their endothelial differentiation *in vitro*. CD31(PECAM-1)$^+$ and CD31^{bright} cells appeared at an early stage of the *in vitro* differentiation of AC133$^+$ cells, and CD31^{bright} cells derived from AC133$^+$ cells were identified as the precursors of endothelial cells because CD31^{bright} cells had differentiated more efficiently to endothelial cells than others. Therefore, we conclude that CD31^{bright} cells derived from AC133$^+$ cells possess the typical character of EPCs. In this study, we analyzed the effects of TPO on the appearance of CD31^{bright} cells from AC133$^+$ cells, and we show that TPO plays an important role in *in vitro* EPC expansion.

EXPERIMENTAL PROCEDURES

Reagents—Recombinant TPO and recombinant stem cell factor (SCF) were kindly provided by Kirin-Amgen Inc. (Thousand Oaks, CA). Recombinant human VEGF was purchased from Strathmann Biotec AG (Hamburg, Germany). The AC133

* This work was supported in part by a grant-in-aid for health and labor science research from the Japanese Ministry of Health, Labor, and Welfare, and in part by a grant-in-aid for Research on Health Sciences focusing on Drug Innovation from the Japan Health Sciences Foundation. The costs of publication of this article were defrayed in part by the payment of page charges. This article must therefore be hereby marked "*advertisement*" in accordance with 18 U.S.C. Section 1734 solely to indicate this fact.

[1] To whom correspondence should be addressed. Tel.: 81-3-3700-9064; Fax: 81-3-3707-6950; E-mail: yamaguch@nihs.go.jp.

[2] The abbreviations used are: EPCs, endothelial precursor cells; VEGF, vascular endothelial growth factor; FN, fibronectin; PBS, phosphate-buffered saline; FITC, fluorescein isothiocyanate; PE, phycoerythrin; TPO, thrombopoietin; SCF, stem cell factor; G-CSF, granulocyte colony-stimulating factor; GM-CSF, granulocyte macrophage-colony stimulating factor; IL, interleukin; PI3K, phosphatidylinositol 3-kinase; VEcad, vascular endothelial cadherin; eNOS, endothelial nitric oxide synthase; FBS, fetal bovine serum; STAT, signal transducers and activators of transcription; JAK, Janus kinase; KDR, kinase insert domain-containing receptor.

magnetic cell sorting kit and phycoerythrin (PE)-conjugated anti-CD133/2 antibody were from Miltenyi Biotec (Gladbach, Germany). Allophycocyanin-conjugated anti-CD110 (TPO receptor) antibody, fluorescein isothiocyanate (FITC)-conjugated anti-CD31 monoclonal antibody, FITC-conjugated anti-CD34 monoclonal antibody, and anti-STAT3 monoclonal antibody were from Pharmingen. Phycoerythrin-conjugated vascular endothelial cadherin (VEcad/CD144) antibody was from Beckman Coulter (Marseilles, France). Anti-vascular endothelial growth factor receptor-2 (Flk-1/KDR) monoclonal antibody (Santa Cruz Biotechnology, Inc., Santa Cruz, CA) and anti-human endothelial nitric oxide synthase (eNOS) rabbit polyclonal antibody (Cayman Chemical, Ann Arbor, MI) were obtained. Anti-phospho-Akt (Ser-473) antibody, anti-Akt antibody, and anti-phospho-STAT3 (Tyr-705) antibody were from Cell Signaling Technology (Beverly, MA). Fibronectin (FN)- and type IV collagen-coated dishes were purchased from Iwaki Co., Tokyo, Japan. Phycoerythrin-conjugated anti-CD14 antibody was from DakoCytomation (Glostrup, Denmark).

Preparation of Peripheral Blood Mononuclear Cells—Human cord blood was kindly supplied by the Metro Tokyo Red Cross Cord Blood Bank (Tokyo, Japan) with informed consent. The buffy coat fraction was prepared from voluntary donated human blood of Saitama Red Cross of Japan (Saitama, Japan). The blood sample was diluted with phosphate-buffered saline (PBS) containing 2 mM EDTA and was loaded on a Lymphoprep™ tube (Axis-Shield PoC AS, Oslo Norway) (density = 1.077). After being centrifuged for 20 min 800 × *g* at 18 °C, mononuclear cells were collected and washed with sorting solution (PBS supplemented with 2 mM EDTA and 0.5% bovine serum albumin).

Flow Cytometric Analysis of AC133 and CD34 Expression in Mononuclear Cells—To eliminate the dead cells, dead cells were stained with 7-amino actinomycin D. Mononuclear cells were labeled with PE-conjugated anti-AC133 monoclonal antibody and FITC-conjugated anti-CD34 monoclonal antibody simultaneously at 4 °C for 30 min. After washing with the sorting solution, flow cytometric analysis was performed with a FACSCalibur (BD Biosciences).

Magnetic Cell Sorting of AC133$^+$ Cells—Mononuclear cells were labeled with magnetic bead-conjugated anti-AC133 antibodies according to the protocol directed by the manufacturer. After the brief wash with the sorting solution, the cells were separated by a magnetic cell separator (autoMACS, Miltenyi Biotec, Gladbach, Germany), and the positive cells were then collected.

Culture of AC133$^+$ Cells—Isolated AC133$^+$ cells were cultured in EBM-2 (Cambrex Corp., East Rutherford, NJ) medium containing 20% heat-inactivated FBS and 30 mg/liter kanamycin sulfate at 37 °C under moisturized air containing 5% CO_2 with 50 ng/ml VEGF as control medium. Control medium containing VEGF was added with TPO, SCF, or both. Cells were plated on FN- or type IV collagen-coated dishes at a cell density of ~10^6 cells/ml. We have previously shown that EPCs can tightly adhere to an FN-coated dish but weakly to type IV collagen-coated dish (25). Analysis of adherent EPCs was performed on FN-coated dish and that of suspended EPCs on type IV collagen-coated dish. Half of the medium was exchanged once every 3–4 days with fresh medium. Adherent cells on FN-coated dish were fixed with ethanol chilled to −20 °C and then subsequently subjected to an immunostaining procedure or other treatments. Cells on type IV collagen-coated dish were subsequently subjected to flow cytometric analysis.

Immunostaining of Adherent Cells—After fixation with chilled ethanol (−20 °C), the cell layer was washed three times with PBS. Cells were incubated with 1% bovine serum albumin in PBS (−) for 1 h at 4 °C for blocking and then with each first antibody in 1% bovine serum albumin in PBS (−) for 1 h at 4 °C. After washing with PBS, the cells were incubated with FITC-conjugated anti-mouse IgG antibody or rhodamine-conjugated anti-rabbit IgG antibody for 1 h at 4 °C. Cells were washed with PBS and then examined using a Zeiss LSM 510 microscope with an excitation wavelength of 488 nm and an emission of 530/30 nm for FITC or 570/30 nm for rhodamine.

In every experiment, we used nonspecific immunoglobulin corresponding to the first antibody species as a control and confirmed that the cells were not stained with control immunoglobulin. The fluorescence intensity of 20 randomly selected cells was calculated using the Scion Image program within the linear range for quantitation.

Analysis of Cytokines in the Supernatant of CD31^{bright} and CD31$^+$ Cells—The expression of CD31 on cultured AC133$^+$ cells was determined with a flow cytometer. After AC133$^+$ cells were cultured for several days on either FN-coated or collagen type IV-coated dishes, both adherent and nonadherent cells were collected. The collected cells were labeled with FITC-labeled anti-CD31 antibody for 15 min at 4 °C. After a brief wash with 0.5% bovine serum albumin in PBS, flow cytometric analysis was performed. CD31^{bright} and CD31$^+$ cells were sorted from cultured AC133$^+$ cells with FACSAria (BD Biosciences). Sorted cells of both populations were subsequently cultured in EBM-2 supplemented with 20% FBS in the absence of any cytokines. After 5 days, the collected supernatant of cells was frozen at −20 °C. Cytokines were measured by a BD™ cytometric beads array Flex set system (BD Biosciences) according to the manufacturer's protocol.

Flow Cytometric Analysis of Various Cell Surface Markers in Cultured AC133$^+$ Cells—After AC133$^+$ cells were cultured for the indicated period, cells were co-stained with FITC-labeled anti-CD31 antibody and PE-labeled anti-CD14 antibody or PE-labeled VEcad antibody. Cells were also stained with FITC-labeled anti-CD31 antibody, allophycocyanin-labeled anti-CD110 antibody, and PE-labeled anti-AC133 antibody triply and then subjected to flow cytometry. Dead cells were eliminated by staining with 7-amino actinomycin D.

Calculation of the Absolute Number of CD31^{bright} Cells—The absolute number of CD31^{bright} cells was multiplied by the total cell number of each well, and the ratio of CD31^{bright} cells was analyzed by fluorescence-activated cell sorter.

Preparation of Cell Lysates and Immunoblotting—After cell sorting, AC133$^+$ cells were suspended in 20% FBS-EBM2 and cultured for 3 days in the presence of VEGF and TPO. Cells were collected and incubated in 2% FBS-EBM2 for 1 h. Cells were stimulated by 50 ng/ml TPO, 50 ng/ml VEGF, or both for 15 min. Cells (1×10^6) were collected and lysed in lysis buffer containing 1% Triton X-100, 10 mM K_2HPO_4/KH_2PO_4 (pH